CANADIAN JOURNAL OF RESEARCH

VOLUME 26 SEPTEMBER, 1948 NUMBER 5

— SECTION A —

PHYSICAL SCIENCES

Contents

NATIONAL RESEARCH COUNCIL
OTTAWA, CANADA

CANADIAN JOURNAL OF RESEARCH

The *Canadian Journal of Research* is issued in six sections, as follows:

A. Physical Sciences	D. Zoological Sciences
B. Chemical Sciences	E. Medical Sciences
C. Botanical Sciences	F. Technology

For the present, Sections A, C, D, and E are to be issued six times annually, and Sections B and F, twelve times annually, each section under separate cover, with separate pagination.

The *Canadian Journal of Research* is published by the National Research Council of Canada under authority of the Chairman of the Committee of the Privy Council on Scientific and Industrial Research. The *Canadian Journal of Research* is edited by a joint Editorial Board consisting of members of the National Research Council of Canada, the Royal Society of Canada, and the Chemical Institute of Canada.

Sections B and F of the *Canadian Journal of Research* have been chosen by the Chemical Institute of Canada as its medium of publication for scientific papers.

Manuscripts should be addressed:

Editor-in-Chief,
Canadian Journal of Research,
National Research Council, Ottawa, Canada.

Canadian Journal of Research

Issued by THE NATIONAL RESEARCH COUNCIL OF CANADA

VOL. 26, SEC. A. SEPTEMBER, 1948 NUMBER 5

THE VIBRATIONAL CONSTANTS OF ACETYLENE[1]

BY NORMA MORGENROTH NORDIN AND R. N. H. HASLAM

Abstract

On the basis of the work done by Darling and Dennison on the water vapor molecule, the vibrational constants of acetylene are calculated, taking into account the resonance interaction arising from the near equality of the fundamentals ν_1 and ν_3. Seventeen band centers are known experimentally. The band centers depend on the 10 constants χ_i, χ_{ik} and γ, which are functions of the potential constants. The expressions for the vibrational energies of the band centers are set up, those for interacting doublets or triplets being found by perturbation methods. The 10 constants are determined and the positions of eight bands calculated to check the results. The agreement is very satisfactory. The positions of 10 other bands not yet observed are predicted.

Introduction

The rotation vibration spectrum of the acetylene molecule has been studied by many investigators such as A. Levin and C. F. Meyer (6), G. Herzberg and J. W. T. Spinks (5), G. W. Funke and G. Herzberg (2), G. Glockler and C. E. Morrell (3), and R. Mecke and R. Ziegler (7). It has been definitely shown from the spectrum that the molecule is linear and symmetrical. There are five normal modes of vibration, shown in Fig. 1.

In the Raman spectrum there are two strong lines at 1973.8 and 3373.7 cm.$^{-1}$, which can be attributed to ν_2 and ν_1 respectively. A weak Raman doublet at 589 and 646 cm.$^{-1}$ has been interpreted as the two branches of the third Raman active vibration, ν_4.

In the infrared two strong absorption bands at 3287 and 729.1 cm.$^{-1}$ are found, and are due to ν_3 and ν_5 respectively. A third band at 1328.1 cm.$^{-1}$ has been interpreted as a combination of ν_4 and ν_5.

It may be noted that some of the earlier authors used different notations. The nomenclature used in this paper is that adopted by Herzberg (4), and not that used by Darling and Dennison (1).

The ordinary and photographic infrared regions have many other combination bands. The assignment of the overtone bands has been the subject of many discussions, one of the latest of these being that given by Wu (8). In all the work done so far there have been discrepancies when constants calculated from some of the bands have been used to calculate positions of other bands.

[1] *Manuscript received March 18, 1948.*

Contribution from the Department of Physics, University of Saskatchewan, Saskatoon, Sask.

It was suggested by Herzberg (4) that these discrepancies might be due to a mutual perturbation of the levels v_1, v_3 and $v_1 - 2$, $v_3 + 2$ with other v's being equal. Since the values of the fundamentals ν_1 and ν_3 are very close together, this perturbation may be expected to be fairly strong.

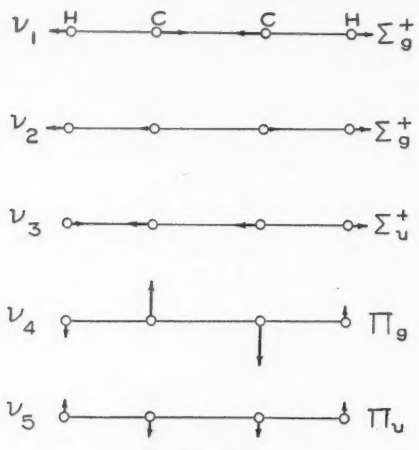

FIG. 1.

This is not a first order resonance effect since ν_1 and ν_3 possess different symmetry properties. In a linear symmetrical molecule the only normal vibrations that may occur are those belonging to the species Σ_g^+, Σ_u^+, π_g and π_u. In the case of acetylene, ν_1 belongs to the species Σ_g^+, and ν_3 to the species Σ_u^+. That is, one is unchanged for reflection at the center of the molecule, and the other changes sign. Therefore the first class is characterized by v_3 being an even integer, and the other by v_3 being odd. Levels that may interact are thus of the type $(v_1, v_2, v_3, v_4, v_5)$ and $(v_1 - 2, v_2, v_3 + 2, v_4, v_5)$. Overtone bands of this type are observed in the spectrum of acetylene, for example, (20100) and (00300) found at 9835.1 and 9639.8 cm.$^{-1}$, and (21100) and (01300) found at 11782.9 and 11600.1 cm.$^{-1}$.

A successful calculation of the energy values of the water vapor molecule, taking into account the resonance between ν_1 and ν_3, has been carried out by Darling and Dennison (1). Although the acetylene molecule is linear, and the water vapor molecule is nonlinear, the calculations for the two are very similar. The method of calculation is as follows.

The expression for the Hamiltonian function is that given by Darling and Dennison, namely,

$$H = \tfrac{1}{2}\sum_{\alpha\beta}\mu^{\frac{1}{4}}(P_\alpha - p_\alpha)\mu_{\alpha\beta}\mu^{-\frac{1}{2}}(P_\beta - p_\beta)\mu^{\frac{1}{4}} + \tfrac{1}{2}\sum_k \mu^{\frac{1}{4}}p_k\mu^{-\frac{1}{2}}p_k\mu^{\frac{1}{4}} + V.$$

The P_α's are the components of the total angular momentum, the p_α's are the components of the vibrational angular momentum, the $\mu_{\alpha\beta}$'s are the components of a determinant μ that contains the moments of inertia; and the p_k's are the momenta conjugate to the normal co-ordinates, q_k.

An expression for the vibrational energy is found, using perturbation theory. To obtain the expression for the energies of perturbing levels in doublets and triplets, the method used is to diagonalize the portion of the Hamiltonian matrix which contains the interacting states.

The Vibrational Energy

For all bands considered, v_4 and v_5 are equal to zero, that is ν_1, ν_2, and ν_3 alone are present. To obtain the position of the band centers the components of the total angular momentum, P_α, are set equal to zero. The remaining Hamiltonian then becomes, as for water vapor:

$$H = \tfrac{1}{2}\sum_k \mu^{\frac{1}{2}} p_k \mu^{-1} p_k \mu^{\frac{1}{2}} + V.$$

The potential V is written as a power series in the normal co-ordinates, and must necessarily be even in q_3.

$$\begin{aligned} V = {} & \tfrac{1}{2}(\lambda_1 q_1^2 + \lambda_2 q_2^2 + \lambda_3 q_3^2) \\ & + \tfrac{1}{2}(a_1 q_1^3 + a_2 q_2^3 + a_3 q_1^2 q_2 + a_4 q_1 q_2^2 + a_5 q_1 q_3^2 + a_6 q_2 q_3^2) \\ & + \tfrac{1}{2}(b_1 q_1^4 + b_2 q_2^4 + b_3 q_3^4 + b_4 q_1^2 q_2^2 + b_5 q_1^2 q_3^2 + b_6 q_2^2 q_3^2). \end{aligned}$$

To obtain the expression for V in terms of the dimensionless variables x_i the following substitutions are made. Since

$$x_i = 2\pi\sqrt{\frac{\omega_i c}{h}}\, q_i$$

we write

$$q_i^2 = \frac{h}{4\pi^2\omega_i c} x_i^2; \qquad \lambda_i = 4\pi^2\omega_i^2 c; \qquad a_i = \frac{hc}{2}\left[\frac{1}{2\pi}\sqrt{\frac{h}{\omega_i c}}\right]^3 \alpha_i$$

and

$$b_i = \frac{hc}{2}\left[\frac{1}{16\pi^4}\cdot\frac{h^2}{\omega_i^2 c^2}\right]\beta_i.$$

The ω_i's are the normal frequencies.

Therefore

$$\begin{aligned} \frac{V}{hc} = {} & \tfrac{1}{2}(\omega_1 x_1^2 + \omega_2 x_2^2 + \omega_3 x_3^2) \\ & + (\alpha_1 x_1^3 + \alpha_2 x_2^3 + \alpha_3 x_1^2 x_2 + \alpha_4 x_1 x_2^2 + \alpha_5 x_1 x_3^2 + \alpha_6 x_2 x_3^2) \\ & + (\beta_1 x_1^4 + \beta_2 x_2^4 + \beta_3 x_3^4 + \beta_4 x_1^2 x_2^2 + \beta_5 x_1^2 x_3^2 + \beta_6 x_2^2 x_3^2). \end{aligned}$$

The quadratic terms constitute the zero order potential, the cubic terms constitute the first order potential, and the quartic terms constitute the second order potential.

The zero order Hamiltonian equation is written

$$H^\circ = \tfrac{1}{2} \sum_{i=1}^{3} p_i^2 + \tfrac{1}{2}hc(\omega_1 x_1^2 + \omega_2 x_2^2 + \omega_3 x_3^2).$$

We replace p_i by

$$\frac{h}{2\pi i}\frac{\partial}{\partial q_i},$$

which is equal to

$$\frac{h}{i}\sqrt{\frac{\omega_i c}{h}}\frac{\partial}{\partial x_i}$$

since

$$\frac{dx_i}{dq_i} = 2\pi\sqrt{\frac{\omega_i c}{h}};$$

p_i^2 is replaced by

$$-h\omega_i c\frac{\partial^2}{\partial x_i^2}$$

and is then allowed to operate on Ψ. Remembering that $H\Psi = W\Psi$ we see that the equation may be written

$$\omega_1\frac{\partial^2\Psi}{\partial x_1^2} + \omega_2\frac{\partial^2\Psi}{\partial x_2^2} + \omega_3\frac{\partial^2\Psi}{\partial x_3^2} + \left(\frac{2W}{hc} - \omega_1 x_1^2 - \omega_2 x_2^2 - \omega_3 x_3^2\right)\Psi = 0$$

If $\Psi = \Psi_1(x_1)$. $\Psi_2(x_2)$. $\Psi_3(x_3)$ and $W = W_1 + W_2 + W_3$ we have three separable equations of the form

$$\frac{d^2\Psi_i}{dx_i^2} + \left(\frac{2W_i}{hc\,\omega_i} - x_i^2\right)\Psi_i = 0 \qquad i = 1, 2, 3$$

The solution of the equation is

$$\Psi_i = N_i e^{-\frac{x_i^2}{2}} H_{v_i}(x_i),$$

where

$$N_i = \left[\frac{1}{\pi^{\frac{1}{2}} 2^{v_i} v_i!}\right]^{\frac{1}{2}}$$

and

$$W_i = hc(v_i + \tfrac{1}{2})\omega_i.$$

The zero order wave function is given by

$$\Psi = Ne^{-\frac{x_1^2}{2}} e^{-\frac{x_2^2}{2}} e^{-\frac{x_3^2}{2}} H_{v_1}(x_1) H_{v_2}(x_2) H_{v_3}(x_3),$$

with

$$N = \left[\frac{1}{\pi^{\frac{3}{2}} 2^{v_1+v_2+v_3} v_1! v_2! v_3!}\right]^{\frac{1}{2}}.$$

The zero order energy W° is written

$$W^\circ = hc[(v_1 + \tfrac{1}{2})\omega_1 + (v_2 + \tfrac{1}{2})\omega_2 + (v_3 + \tfrac{1}{2})\omega_3].$$

$\frac{W^\circ}{hc}$ is usually replaced by G°. Therefore,

$$G^\circ = \tfrac{1}{2}(\omega_1 + \omega_2 + \omega_3) + v_1\omega_1 + v_2\omega_2 + v_3\omega_3.$$

The first order correction to the energy is given by

$$W' = \int \Psi^* H' \Psi d\tau = \int H' \Psi^2 d\tau,$$

where

$$H' = hc[\alpha_1 x_1^3 + \alpha_2 x_2^3 + \alpha_3 x_1^2 x_2 + \alpha_4 x_1 x_2^2 + \alpha_5 x_1 x_3^2 + \alpha_6 x_2 x_3^2].$$

Therefore

$$G' = N^2 \int (\alpha_1 x_1^3 + \ldots + \alpha_6 x_2 x_3^2)\, e^{-x_1^2} e^{-x_2^2} e^{-x_3^2}\, H_{v_1}^2 H_{v_2}^2 H_{v_3}^2 dx_1 dx_2 dx_3$$

Upon integrating, each term is found to be equal to zero, hence the first order correction to the energy is zero.

The second order correction to the energy is given by

$$W'' = \int H'' \Psi^2 d\tau + \sum_{a \neq b} \frac{\left\{\int \Psi_a H' \Psi_b d\tau\right\}^2}{W_a^o - W_b^o},$$

Ψ_a is the wave function for the state (v_1, v_2, v_3).
Ψ_b is the wave function for the state (u_1, u_2, u_3).

$$H'' = hc[\beta_1 x_1^4 + \beta_2 x_2^4 + \beta_3 x_3^4 + \beta_4 x_1^2 x_2^2 + \beta_5 x_1^2 x_3^2 + \beta_6 x_2^2 x_3^2].$$

The first term when integrated gives

$$\begin{aligned}\frac{1}{hc}\int H'' \Psi^2 d\tau &= \frac{3}{2}(\beta_1 v_1^2 + \beta_2 v_2^2 + \beta_3 v_3^2) + \frac{v_1}{2}(3\beta_1 + \beta_4 + \beta_5) \\ &+ \frac{v_2}{2}(3\beta_2 + \beta_4 + \beta_6) + \frac{v_3}{2}(3\beta_3 + \beta_5 + \beta_6) + \beta_4 v_1 v_2 \\ &+ \beta_5 v_1 v_3 + \beta_6 v_2 v_3 + \frac{3}{4}(\beta_1 + \beta_2 + \beta_3) + \frac{1}{4}(\beta_4 + \beta_5 + \beta_6).\end{aligned}$$

The second term is expanded into the expression

$$\sum_{a \neq b} \frac{hc\left\{\int \Psi_a \alpha_1 x_1^3 \Psi_b d\tau + \int \Psi_a \alpha_2 x_2^3 \Psi_b d\tau + \ldots + \int \Psi_a \alpha_6 x_2 x_3^2 \Psi_b d\tau\right\}^2}{W_a^o - W_b^o}.$$

Each integral is considered separately and the values of (u_1, u_2, u_3) which give a nonzero result are found. Let I_1 represent $\int \Psi_a \alpha_1 x_1^3 \Psi_b d\tau$, and I_2 represents $\int \Psi_a \alpha_2 x_2^3 \Psi_b d\tau$. Each integral is found to have nonzero values for four sets of u-values. I_3, I_4, I_5, and I_6 representing the terms in α_3, α_4, α_5, and α_6 respectively, each are found to have nonzero values for six sets of u-values.

The I's for the same values of u_1, u_2, u_3 must be collected and substituted into $\sum_{a \neq b} \frac{\left\{\int \Psi_a H' \Psi_b d\tau\right\}^2}{W_a^\circ - W_b^\circ}$ which gives rise to 24 terms. After squaring and collecting, the terms with equal powers of the v's are collected. The result added to the term $\int H'' \Psi^2 d\tau$ gives the second order correction to the energy.

The complete expression for the energy may be written

$$G = G_o + X_1 v_1 + X_2 v_2 + X_3 v_3 + X_{11} v_1^2 + X_{22} v_2^2 + X_{33} v_3^2 + X_{12} v_1 v_2 + X_{13} v_1 v_3 + X_{23} v_2 v_3$$

G_o is the summation of all constant terms: X_i, X_{ii}, and X_{ik} have the same form as for water vapor (1, p. 132).

The Resonance Interaction in Doublets

The consideration of the resonance interaction between the states (v_1, v_2, v_3) and ($v_1 - 2$, v_2, $v_3 + 2$) does not affect the calculation of the constants. The determinant containing the interacting states for a doublet is

$$\begin{vmatrix} H_{kk} - G, & H_{kJ} \\ H_{Jk}, & H_{JJ} - G \end{vmatrix} = 0.$$

k refers to the state (v_1, v_2, v_3) and J to the state ($v_1 - 2$, v_2, $v_3 + 2$).

$$H_{kk} = \int \Psi_k^* \overline{H} \Psi_k d\tau \qquad \text{and} \qquad H_{kJ} = H_{Jk} = \int \Psi_k^* \overline{H} \Psi_J d\tau.$$

$\overline{H}$ is the total Hamiltonian, and to a second order approximation is given by

$$\overline{H} = H^\circ + \lambda H' + \lambda^2 H''.$$

To the same order of approximation Ψ_k is given by

$$\Psi_k = \Psi_k^\circ + \lambda \Psi_k' = \Psi_k^\circ + \lambda \sum_{m \neq k} \frac{\int \Psi_m^{\circ *} H' \Psi_k^\circ d\tau}{W_k^\circ - W_m} \cdot \Psi_m^\circ \cdot$$

Similarly

$$\Psi_J = \Psi_J^\circ + \lambda \sum_{P \neq J} \frac{\int \Psi_P^{\circ *} H' \Psi_J^\circ d\tau}{W_J^\circ - W_P^\circ} \cdot \Psi_P^\circ \cdot$$

The expression for H_{kJ} is given by

$$\int [\Psi_k^{\circ *} + \lambda \sum_{m \neq k} A_m \Psi_m^{\circ *}] [H^\circ + \lambda H' + \lambda^2 H''] [\Psi_J^\circ + \lambda \sum_{P \neq J} A_P \Psi_P^\circ] d\tau.$$

In the expansion, terms are taken to only a second order approximation.

$$H_{kJ} = \int \Psi_k^{\circ *} H'' \Psi_J^\circ d\tau + \sum_{m \neq k} A_m \int \Psi_m^{\circ *} H' \Psi_J^\circ d\tau + \sum_{P \neq J} A_P \int \Psi_k^{\circ *} H' \Psi_P^\circ d\tau.$$

The first term, given by

$$N_k N_J \int (\beta_1 x_1^4 + \ldots + \beta_6 x_2^2 x_3^2) e^{-x_1^2} e^{-x_2^2} e^{-x_3^2} H_{v_1} H_{v_1-2} H_{v_2}^2 H_{v_3} H_{v_3+2} dx_1 dx_2 dx_3 ,$$

upon integration reduces to

$$\tfrac{1}{4}\beta_5 [v_1(v_1 - 1)\,(v_3 + 1)\,(v_3 + 2)]^{\frac{1}{2}} .$$

The second term consists of two factors, each depending on H'.

$$\sum_{m \neq k} A_m \int \Psi_m^{\circ *} H' \Psi_j^\circ d\tau = \sum_{m \neq k} \frac{\int \Psi_m^{\circ *} H' \Psi_k^\circ d\tau}{W_k^\circ - W_m^\circ} \cdot \int \Psi_m^{\circ *} H' \Psi_j^\circ d\tau .$$

The terms in each factor having the same v-values give rise to nonzero products. The resonance between ν_1 and ν_3 is due to the near equality of the fundamental frequencies ω_1 and ω_3. These frequencies may be assumed to be equal in a second order approximation. When ω_3 is replaced by ω_1, the expression for

$$\sum_{m \neq k} A_m \int \Psi_m^{\circ *} H' \Psi_j^\circ d\tau$$

becomes

$$\left[v_1(v_1 - 1)\,(v_3 + 1)\,(v_3 + 2)\right]^{\frac{1}{2}} \left[-\frac{1}{2}\frac{\alpha_5^2}{\omega_1} + \frac{1}{4}\frac{\alpha_1\alpha_5}{\omega_1} + \frac{1}{8}\frac{\alpha_3\alpha_6}{(2\omega_1 - \omega_2)} - \frac{1}{8}\frac{\alpha_3\alpha_6}{(2\omega_1 + \omega_2)}\right].$$

The third term,

$$\sum_{P \neq J} A_P \int \Psi_k^{\circ *} H' \Psi_P^\circ d\tau ,$$

gives the same result. Thus

$$H_{kJ} = \left[v_1(v_1 - 1)\,(v_3 + 1)\,(v_3 + 2)\right]^{\frac{1}{2}} \left[\frac{1}{4}\beta_5 - \frac{\alpha_5^2}{\omega_1} + \frac{1}{2}\frac{\alpha_1\alpha_5}{\omega_1} + \frac{1}{4}\frac{\alpha_3\alpha_6}{(2\omega_1 - \omega_2)} - \frac{1}{4}\frac{\alpha_3\alpha_6}{(2\omega_1 + \omega_2)}\right].$$

$$= \tfrac{1}{2}\gamma \left[v_1(v_1 - 1)\,(v_3 + 1)\,(v_3 + 2)\right]^{\frac{1}{2}},$$

where the interaction constant γ is given by

$$\gamma = \frac{1}{2}\beta_5 - \frac{2\alpha_5^2}{\omega_1} + \frac{\alpha_1\alpha_5}{\omega_1} + \frac{\alpha_3\alpha_6}{2(2\omega_1 - \omega_2)} - \frac{\alpha_3\alpha_6}{2(2\omega_1 + \omega_2)} .$$

This is the expression given by Darling and Dennison (1, p. 133) except for a factor of 2 in the α-terms (which however does not affect the following calculations).

Then to obtain the energy of the components of a doublet, the following determinantal equation must be solved

$$\begin{vmatrix} H_{kk} - G, & \frac{b}{hc} \\ \frac{b}{hc}, & H_{JJ} - G \end{vmatrix} = 0,$$

where

$$b = hcH_{kJ} = \tfrac{1}{2}hc\gamma[v_1(v_1 - 1)\,(v_3 + 1)\,(v_3 + 2)]^{\frac{1}{2}}$$

This may be written

$$G^2 - G(H_{kk} + H_{JJ}) - \left(\frac{b}{hc}\right)^2 + H_{kk}H_{JJ} = 0.$$

The solution is

$$G = \frac{(H_{kk} + H_{JJ}) \pm \sqrt{\left(H_{kk} - H_{JJ}\right)^2 + \left(\frac{2b}{hc}\right)^2}}{2}.$$

The roots are thus the average of the unperturbed levels, plus or minus—one-half the square root of (the square of the difference of the unperturbed levels, plus the square of the separation due to the interaction).

The Resonance Interaction in Triplets

To obtain the roots of a triplet (v_1, v_2, v_3), $(v_1 - 2, v_2, v_3 + 2)$, $(v_1 - 4, v_2, v_3 + 4)$ the determinant containing the interacting states must be solved.

$$\begin{vmatrix} H_{kk} - G, & H_{kJ}, & H_{kR} \\ H_{Jk}, & H_{JJ} - G, & H_{JR} \\ H_{Rk}, & H_{RJ}, & H_{RR} - G \end{vmatrix} = 0$$

k refers to the state (v_1, v_2, v_3), J to the state $(v_1 - 2, v_2, v_3 + 2)$, and R to the state $(v_1 - 4, v_2, v_3 + 4)$. The expression for $H_{kJ} = H_{Jk}$ has already been found. A similar calculation gives an expression for $H_{JR} = H_{RJ}$.

$$H_{JR} = \int \Psi_J^{\circ *} H'' \Psi_R^{\circ} d\tau + \sum_{m \neq J} A_m \int \Psi_m^{\circ *} H' \Psi_R^{\circ} d\tau + \sum_{P \neq R} A_P \int \Psi_J^{\circ *} H' \Psi_P^{\circ} d\tau .$$

Ψ_J° and Ψ_R° have the usual form, and A_m and A_P are given by

$$A_m = \frac{\int \Psi_m^{\circ *} H' \Psi_J^{\circ} d\tau}{W_J^{\circ} - W_m^{\circ}} \; ; \qquad A_P = \frac{\int \Psi_P^{\circ *} H' \Psi_R^{\circ} d\tau}{W_R^{\circ} - W_P^{\circ}}$$

The calculation is exactly similar to that for doublets, with v_1 replaced by $v_1 - 2$ and v_3 replaced by $v_3 + 2$.

Thus

$$H_{JR} = H_{RJ} = \tfrac{1}{2}\gamma[(v_1 - 2)(v_1 - 3)(v_3 + 3)(v_3 + 4)]^{\frac{1}{2}}.$$

The expression for H_{kR} is given by

$$H_{kR} = \int \Psi_k^{\circ *} H' \Psi_R^{\circ} d\tau + \sum_{m \neq k} A_m \int \Psi_m^{\circ *} H' \Psi_R^{\circ} d\tau + \sum_{P \neq R} A_P \int \Psi_k^{\circ *} H' \Psi_P^{\circ} d\tau .$$

All terms when integrated are equal to zero. Hence $H_{kR} = H_{Rk} = 0$. The determinantal equations may be written

$$\begin{vmatrix} H_{kk} - G, & \frac{b}{hc}, & 0 \\ \frac{b}{hc}, & H_{JJ} - G, & \frac{a}{hc} \\ 0, & \frac{a}{hc}, & H_{RR} - G \end{vmatrix} = 0$$

$$b = \tfrac{1}{2}hc\gamma[v_1(v_1 - 1)(v_3 + 1)(v_3 + 2)]^{\frac{1}{2}}$$

and

$$a = \tfrac{1}{2}hc\gamma[(v_1 - 2)(v_1 - 3)(v_3 + 3)(v_3 + 4)]^{\frac{1}{2}}.$$

Thus

$$G^3 - [H_{kk} + H_{JJ} + H_{RR}]G^2 + \left[H_{kk}H_{JJ} + H_{JJ}H_{RR} + H_{RR}H_{kk} - \left(\frac{a}{hc}\right)^2 - \left(\frac{b}{hc}\right)^2\right]G - H_{kk}H_{JJ}H_{RR} + \left(\frac{b}{hc}\right)^2 H_{RR} + \left(\frac{a}{hc}\right)^2 H_{kk} = 0.$$

Knowing the constants and the v-values for any triplet, a cubic equation may be set up and the roots found by approximation.

The Numerical Results

Seventeen bands of acetylene whose positions are known are shown in Table I. Nine of the bands were used to calculate the force constants, X_i and X_{ik}, taking no account of the resonance interaction. These are marked

TABLE I

v_1	v_2	v_3	Position, cm.$^{-1}$	v_1	v_2	v_3	Position, cm.$^{-1}$
0	1	0	1973.8*	0	1	3	11600.1*
0	0	1	3287.0*	2	1	1	11782.9*
1	0	0	3373.7*	1	0	3	12675.7
1	1	1	8512.1*	0	2	3	13532.4
0	3	1	9151.7*	1	1	3	14617.0
0	1	1	5250	0	0	5	15600.2
1	0	1	6500	0	1	5	17518.8
0	0	3	9639.8*	1	0	5	18430.2
2	0	1	9835.1*				

with an asterisk. The two with the v-values of (011) and (101) were not used in the calculations as these were measured with very small dispersion and thus their positions are not well known.

The values of the constants were thus found to be,

$X_1 = 3366.2$ cm.$^{-1}$ $\quad X_{11} = 7.5$ cm.$^{-1}$ $\quad X_{12} = -10.75$ cm.$^{-1}$

$X_2 = 1981.0$ " $\quad X_{22} = -7.2$ " $\quad X_{13} = -107.15$ "

$X_3 = 3323.87$ " $\quad X_{33} = -36.87$ " $\quad X_{23} = -4.5$ "

It is evident that if the resonance interaction is considered an additional band will be needed to evaluate the X_i's and X_{ik}'s and γ, the interaction constant. The equations used are given below. For doublets, the general expression

$$G = \tfrac{1}{2}(H_{kk} + H_{JJ}) \pm \tfrac{1}{2}\sqrt{\left(H_{kk} - H_{JJ}\right)^2 + \left(\frac{2b}{hc}\right)^2}$$

was used to derive the equations.

v_1	v_2	v_3		
0	1	0	$X_2 + X_{22} = 1973.8$	(1)
0	0	1	$X_3 + X_{33} = 3287.0$	(2)
1	0	0	$X_1 + X_{11} = 3373.7$	(3)
1	1	1	$X_1 + X_{11} + X_2 + X_{22} + X_3 + X_{33} + X_{12} + X_{13} + X_{23} = 8512.1$	(4)
0	3	1	$3X_2 + 9X_{22} + X_3 + X_{33} + 3X_{23} = 9151.7$	(5)
2	0	1	$X_1 + 2X_{11} + 2X_3 + 5X_{33} + X_{13} + \tfrac{1}{2}\sqrt{(2X_1 + 4X_{11} - 2X_3 - 8X_{33} + 2X_{13})^2 + 12\gamma^2} = 9835.1$	(6)
0	0	3	$X_1 + 2X_{11} + 2X_3 + 5X_{33} + X_{13} - \tfrac{1}{2}\sqrt{(2X_1 + 4X_{11} - 2X_3 - 8X_{33} + 2X_{13})^2 + 12\gamma^2} = 9639.8$	(7)
2	1	1	$X_1 + 2X_{11} + X_2 + X_{22} + 2X_3 + 5X_{33} + X_{12} + X_{13} + 2X_{23} + \tfrac{1}{2}\sqrt{(2X_1+4X_{11}-2X_3-8X_{33}+2X_{12}+2X_{13}-2X_{23})^2+12\gamma^2} = 11782.9$	(8)
0	1	3	$X_1 + 2X_{11} + X_2 + X_{22} + 2X_3 + 5X_{33} + X_{12} + X_{13} + 2X_{23} - \tfrac{1}{2}\sqrt{(2X_1+4X_{11}-2X_3-8X_{33}+2X_{12}+2X_{13}-2X_{23})^2+12\gamma^2} = 11600.1$	(9)
1	0	3	$2X_1 + 5X_{11} + 2X_3 + 5X_{33} + 3X_{13} - \tfrac{1}{2}\sqrt{(2X_1 + 8X_{11} - 2X_3 - 8X_{33})^2 + 36\gamma^2} = 12675.7$	(10)

Some difficulty was encountered in the solution of these 10 equations. The first nine can be reduced to the following two equations,

$$(-12X_{33} - 247.1)^2 + 12\gamma^2 = (195.3)^2.$$

$$[-12X_{33} - 247.1 - 2(-19.75 - 3X_{23})]^2 + 12\gamma^2 = (182.8)^2$$

These can most easily be solved by assigning an arbitrary value to one of the three unknowns. The value of X_{23} was varied, and the constants were determined each time and substituted into Equation (10) to find the best check with the observed position of this band. When $X_{23} = +3$ the calculated position of the band is 12675.6 cm.$^{-1}$, the observed position is 12675.7 cm.$^{-1}$, so this value of X_{23} was used. The constants are now

$$X_1 = 3405.1 \text{ cm.}^{-1} \quad X_{11} = -31.4 \text{ cm.}^{-1} \quad X_{12} = -25.75 \text{ cm.}^{-1}$$
$$X_2 = 1984.75 \text{ "} \quad X_{22} = -10.95 \text{ "} \quad X_{13} = -99.65 \text{ "}$$
$$X_3 = 3313.4 \text{ "} \quad X_{33} = -26.4 \text{ "} \quad X_{23} = +3.0 \text{ "}$$
$$12\gamma^2 = 33267 \qquad |\gamma| = 52.65$$

When the positions of the bands (011), (101), (023), and (113) are calculated, the values are found to agree favorably with the observed positions.

In the spectrum of acetylene there are also found three bands each of which is one root of a triplet. They are the bands (005), (015), and (105) found at 15600.2, 17518.8, and 18430.2 cm.$^{-1}$ respectively.

The determinant for each triplet was set up and solved. The results are given below.

The triplet (401), (203), and (005) has the determinant

$$\begin{vmatrix} H_{kk} - G, & 3\sqrt{2}.\gamma & 0 \\ 3\sqrt{2}.\gamma & H_{JJ} - G, & \sqrt{10}.\gamma \\ 0, & \sqrt{10}.\gamma & H_{RR} - G \end{vmatrix} = 0$$

$H_{kk} = 4X_1 + 16X_{11} + X_3 + X_{33} + 4X_{13} = 16006.4$
$H_{JJ} = 2X_1 + 4X_{11} + 3X_3 + 9X_{33} + 6X_{13} = 15789.3$
$H_{RR} = 5X_3 + 25X_{33} = 15907.0$
The roots were found to be 15633.8, 15841.51, and 16223.42 cm.$^{-1}$

For the triplet (411), (213), (015) the determinant has the same form, but the H's are now

$H_{kk} = 4X_1 + 16X_{11} + X_2 + X_{22} + X_3 + X_{33} + 4X_{13} + 4X_{12} + X_{23} = 17880.2$
$H_{JJ} = 2X_1 + 4X_{11} + X_2 + X_{22} + 3X_3 + 9X_{33} + 2X_{12} + 6X_{13} + 3X_{23} = 17720.6$
$H_{RR} = X_2 + X_{22} + 5X_3 + 25X_{33} + 5X_{23} = 17895.8.$
The roots are 17516.78, 17867.2, and 18097.23 cm.$^{-1}$

The determinant for the third triplet, (501), (303), (105), is

$$\begin{vmatrix} H_{kk} - G, & \sqrt{30}.\gamma & 0 \\ \sqrt{30}.\gamma & H_{JJ} - G, & \sqrt{30}.\gamma \\ 0, & \sqrt{30}.\gamma & H_{RR} - G \end{vmatrix} = 0$$

$$H_{kk} = 5X_1 + 25X_{11} + X_3 + X_{33} + 5X_{13} = 19029.25$$
$$H_{JJ} = 3X_1 + 9X_{11} + X_3 + 9X_{33} + 9X_{13} = 18738.45$$
$$H_{RR} = X_1 + X_{11} + 5X_3 + 25X_{33} + 5X_{13} = 18782.45.$$

The roots are 18370.73, 18926.05, and 19235.19 cm.$^{-1}$

There is no way of distinguishing between the v-values for the observed band of each triplet, since the perturbation makes each level a mixture of all three unperturbed levels. One unperturbed level may be said to predominate in each root.

Using the values of the constants found in this paper, the positions of 10 bands not yet observed were predicted. These values are shown in Table II,

TABLE II

A SUMMARY OF THE RESULTS

v_1	v_2	v_3	Observed position, cm.$^{-1}$	Calculated values	
				No resonance interaction	With resonance interaction
0	1	0	1973.8		
0	0	1	3287.0		
1	0	0	3373.7		
1	1	1	8512.1		
0	3	1	9151.7		
0	1	1	5250	5256.3	5263.8
1	0	1	6500	6553.65	6561.05
0	0	3	9639.8		
2	0	1	9835.1		
0	1	3	11600.1		
2	1	1	11782.9		
1	0	3	12675.7	12692.03	12675.6
3	0	1	—		13022.5
0	2	3	13532.4	13545.98	13530.7
2	2	1	—		13716.6
1	1	3	14617.0	14641.58	14613.65
3	1	1	—		14941.05
1	1	2	—		11611.7
3	1	0	—		11867.2
1	0	3	—		9152.15
1	3	1	—		12348.5
1	1	0	—		5321.75
0	3	3	—		15429.2
2	3	1	—		15638.6
4	0	1	15600.2	16443.2	15633.8
2	0	3		15759.28	
0	0	5		15697.6	
4	1	1	17518.8	18369.5	17516.78
2	1	3		17698.08	
0	1	5		17648.9	
5	0	1	18430.2	19769.75	18370.73
3	0	3		18841.53	
1	0	5		18535.55	

which gives a summary of all the results. The observed positions of all bands, including the three belonging to triplets, are shown in the second column. In the third column the values are calculated using the constants

found when no resonance interaction is considered. For each of the three triplets, three values are recorded corresponding to the three sets of v-values. In the fourth column the values are calculated using the constants found when the resonance interaction is considered. For the triplets only the one root closest to the observed value is recorded, since no one root can be identified wholly with any one set of v-values.

By comparing the calculated values with the observed values it is quite evident that the agreement for the fourth column is much more marked than for the third column. Thus the results justify the assumption that the previous discrepancies in the work on acetylene were due to the mutual perturbation of the levels $(v_1, v_2, v_3, v_4, v_5)$ and $(v_1 - 2, v_2, v_3 + 2, v_4, v_5)$. That the perturbation consideration may be carried on to triplets is a further justification of the assumption.

Acknowledgment

The authors wish to express their thanks to Dr. G. Herzberg for suggesting that this calculation be carried out, and for much valuable assistance.

References

1. DARLING, B. T. and DENNISON, D. M. Phys. Rev. 57 : 128. 1940.
2. FUNKE, G. W. and HERZBERG, G. Phys. Rev. 49 : 100. 1936.
3. GLOCKLER, G. and MORRELL, C. E. J. Chem. Phys. 4 : 15. 1936.
4. HERZBERG, G. Infrared and Raman spectra of polyatomic molecules. Vol. 2 of Molecular spectra and molecular structure. D. Van Nostrand Company, Inc., New York. 1945.
5. HERZBERG, G. and SPINKS, J. W. T. Z. Physik, 91 : 386. 1934.
6. LEVIN, A. and MEYER, C. F. J. Optical Soc. Am. 16 : 137. 1928.
7. MECKE, R. and ZIEGLER, R. Z. Physik, 101 : 405. 1936.
8. WU, T. Vibrational spectra and structure of polyatomic molecules. National University of Peking, Peiping, China. G. E. Stechert & Company, New York, London. 1939.

SENSITIVITY AND EXPOSURE GRAPHS FOR RADIUM RADIOGRAPHY[1]

By H. E. Johns and C. Garrett[2]

Abstract

The radiography of steel by the use of the gamma rays from radium is discussed. The thickness of lead front screen which yields the maximum intensifying effect is determined and the action of the front screen discussed. Sensitivity curves are obtained using a slotted wedge steel penetrameter for a number of the commonly used types of X-ray film. It is shown that the thickness of the lead front screen which produces the maximum density on the film is not necessarily the most useful thickness for gamma radiography. The most useful thickness is determined from penetrameter sensitivity curves. The importance of these sensitivity curves for routine gamma ray testing is indicated.

Introduction

Several methods have been used in the past for the selection of the proper exposure factor required to give a suitable radiograph of a casting. The method developed in the National Research Council by Laurence, Ball, and Archibald (1) has been found very satisfactory for X-rays. The basis of the method is a wedge penetrameter (see Fig. 3) in which slots have been cut whose depth at any point is a constant percentage of the thickness of the wedge. Slots of depth 1, 2, 3, 5, and 10% are usually sufficient for the adequate testing of a film. This wedge penetrameter is then X-rayed for a series of exposures and the films developed in a standard way (2). Examinations of such films will reveal that the 2% slot is observable for a certain range of thicknesses of the wedge and for a certain range of exposure factors. This will be discussed in detail later.

This method, which has been developed primarily for use in X-ray work, has been extended by the authors to the field of gamma radiography. For gamma radiography Nodwell and Morrison (2) have measured the densities obtainable with a selection of films for different exposure factors. Although their results are of considerable use and interest, the authors feel that differential sensitivity (i.e., a knowledge that a flaw of a given percentage thickness will be made visible) is of much greater importance. It is customary in taking radiographs to use a lead front screen and a thicker lead back screen. These lead screens produce a certain amount of intensification (i.e., increase in density for a given exposure factor) and also reduce the blurring effect of scattered radiation. It is found that a certain thickness of lead front screen produces the maximum density for a given thickness of casting. It does not follow that this "optimum" thickness will give also the greatest differential sensitivity. This latter question can be answered by the use of the wedge penetrameter. The intensification of the front screen will be discussed first and then the sensitivity curves.

[1] *Manuscript received May 4, 1948.*
Contribution from the Physics Department, University of Saskatchewan, Saskatoon, Sask.
[2] *Holder of a Bursary under the National Research Council of Canada.*

The Optimum Thickness of Lead Front Screens

In what follows in this section the "optimum" thickness of front screen will be defined as the thickness which produces the maximum density on the film. Later we will see that this is not the sole criterion for the choice of a front screen.

To find this "optimum" thickness a series of steel blocks from 0.5 to 3.0 in. thick were radiographed using a step wedge front screen made up of sheets of lead having thicknesses of 0.001, 0.002, 0.003, 0.006, 0.012, 0.018, 0.024, and 0.030 in. in immediate contact with the film and separated from the steel by the standard Kodak cardboard film holder. A series of radiographs with different exposure factors was taken using "No Screen" film backed by 0.030 in. of lead. The radium was held in a brass cup of wall thickness 0.125 in. The films were developed in Kodalk for five minutes at 20° C. and standard agitation was carried out (2). Densities were measured on a Marshall densitometer and are plotted against exposure factor (mgm. × min. per in.²) as in Fig. 1. (Film of density 1.0 will transmit 0.1 of the incident light; film of density 2.0 will transmit 0.01 of the incident light.)

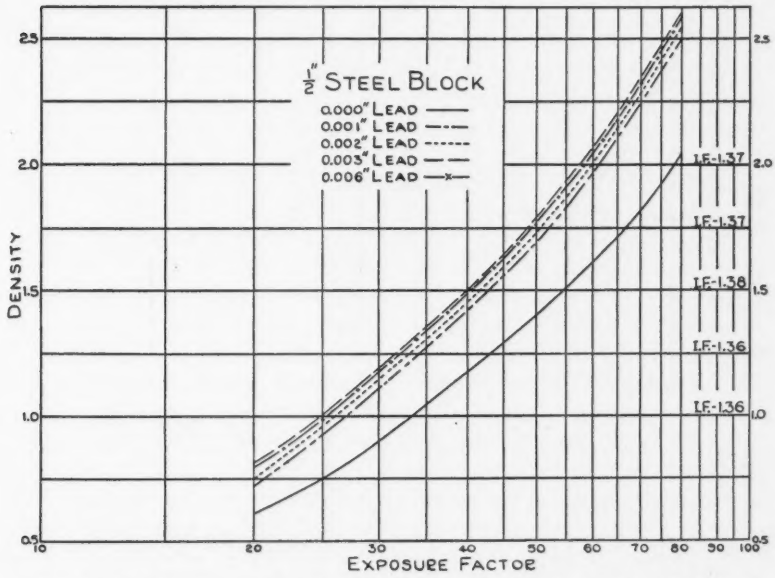

FIG. 1. *Density versus exposure factor for "No Screen" film, developed in "Kodalk" at 20° C. for five minutes with standard agitation. Radium filter, 0.125 in. brass. Back screen, 0.030 in. of lead in contact with the film. Front lead screen as indicated.*

The intensification factor due to the front screen is defined as the ratio of two exposure factors, the first made with no lead front screen and the second made with a lead front screen, in such a way as to produce an equal density on

the film. For example from Fig. 1 we see that density 1.0 requires an exposure factor of 34.0 when no lead front screen is used and 25.0 when a 0.003 in. lead front screen is used. The intensification factor is therefore 1.36. For densities 1.25, 1.50, 1.75, and 2.00 the intensification factors are 1.36, 1.38, 1.37, and 1.37 respectively, giving an average of 1.37. In a similar way the intensification factors for other thicknesses of the lead front screens and other thicknesses of steel block were obtained. These are shown graphically in Fig. 2. It will be seen that as the thickness of the steel block is increased the

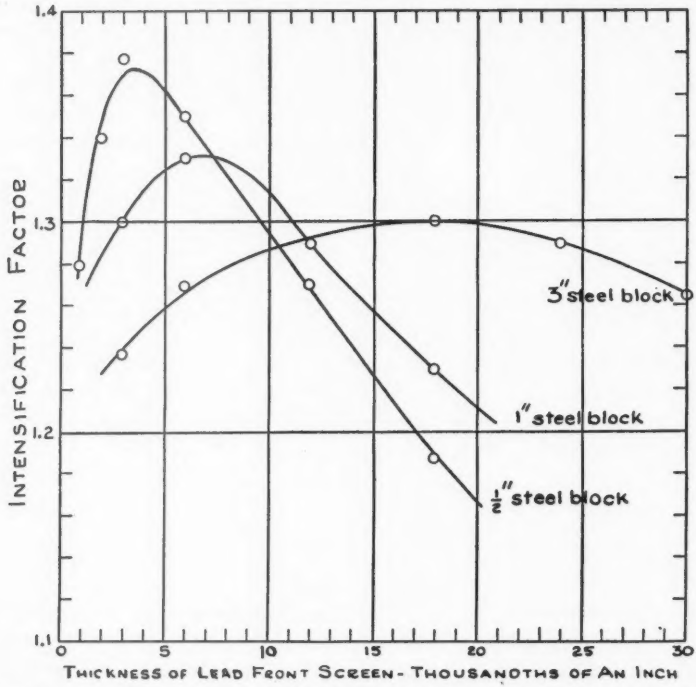

FIG. 2. *Intensification factor versus thickness of lead front screen for steel, 1/2, 1, and 3 in. thick.*

"optimum" thickness of lead front screen also increases. At the same time the actual value of the maximum intensification obtainable decreases slightly. If the optimum thickness of lead front screen is plotted against the thickness of steel block a linear relation will result. For example the optimum thicknesses of lead front screens are 0.003, 0.006, 0.012, 0.018 in. for steel of thicknesses 0.5, 1.0, 2.0, and 3.0 in. respectively.

To give further information concerning the actual action of the lead intensifying screen the following experiments were carried out using a 0.50 in. steel block and "No Screen" film. Results similar to those shown in Fig. 1

were obtained for a number of different arrangements of steel, lead, Kodak cardboard film holder, and film as indicated below. From these it was found that density 1.50 was obtained for the exposure factors given below.

(*a*) The steel was separated from the film by the cardboard film holder. Exposure factor, *54.8*.

(*b*) The steel was placed in *direct* contact with the film. Exposure factor, *49.8*

(*c*) The steel was placed immediately against the lead front screen (0.003 in. lead) which was in contact with the film. Exposure factor, *40.2*.

(*d*) The steel was placed on the film holder and the lead front screen (0.003 in. lead) was in direct contact with the film inside the film holder. Exposure factor, *40.0*.

The exposure factors for (*c*) and (*d*) are essentially the same, as one would expect owing to the negligible absorption of the gamma rays in the cardboard film holder. (*b*) gives an intensification of 1.10 over (*a*). This means that a steel front screen would give an intensification of approximately 1.10. (*c*) and (*d*) give an intensification of 1.36 over (*a*).

The reason for this general behavior of lead front screens can be seen from the following considerations. At the lower face of the steel block there is equilibrium between the electrons (photoelectrons and Compton electrons) and the electromagnetic radiation (gamma rays, Compton scattered radiation, and fluorescent radiation) all characteristic of steel. The cardboard film holder will absorb for practical purposes all the electrons from the steel and in their place will appear the corresponding electrons from cardboard. If a sheet of lead is inserted between the film and cardboard whose thickness is equal to the maximum range R of the electrons, then all the electrons from the cardboard will be stopped and in their place will appear the electrons originating in the lead. Since gamma rays from Radium C eject essentially the same number of Compton electrons from equal masses of cardboard and lead, the intensification must be due mainly to photoelectrons. The photoelectric absorption by lead is greater than by cardboard, so more photoelectrons will be produced in the lead foil than were stopped, giving a net intensifying action. When the steel block is placed in *direct* contact with the film there is an increase in density over that when the cardboard casette is used but a decrease in density as compared with the use of the cardboard casette and the lead front screen. This result is of course due to the photoelectric absorption being greater in lead than in steel. If a lead casting were being radiographed no increase in density would result by the use of a lead front screen if the casting could be placed in direct contact with the film.

If the lead front screen is thicker than R the electrons produced at the front of the screen will be stopped before they reach the film anyway, and only those produced within the range R of the back of the intensifying screen can

affect the film. The front part of the foil has merely served to reduce the intensity of the gamma rays, so a reduction in the intensifying action results. This general picture serves to explain also why a thicker front screen is needed for thicker pieces of steel. As the steel thickness is increased, the softer components from the radium are filtered out and the average range of the photoelectrons produced increases. The maxima in Fig. 2 are however broad because of the inhomogeneity of the gamma rays from radium, and because the electrons are not all ejected in the forward direction, nor from the same depth.

Penetrameter Sensitivities of Different Types of X-Ray Films

In the last section the thickness of lead front screen which produced the maximum density was considered as "optimum", but one is primarily interested in the penetrameter sensitivity or differential sensitivity (i.e., a knowledge that a flaw of a given percentage thickness will be made visible). This was obtained by the method described by Laurence, Ball, and Archibald (1) for several types of X-ray films and the variation of this sensitivity with the thickness of the lead front screen measured. All films were developed in Kodalk at 20° C. for five minutes and given standard agitation (2). The radiation from the radium was filtered by 0.125 in. of brass in all cases. The films were viewed using the methods outlined in (1).

A steel wedge suitable for gamma radiography, 10 in. long, 4 in. wide, and of maximum thickness 4 in. was made and is illustrated in Fig. 3. When radiographs of such a wedge are taken using a distance from source to film of 24 in.

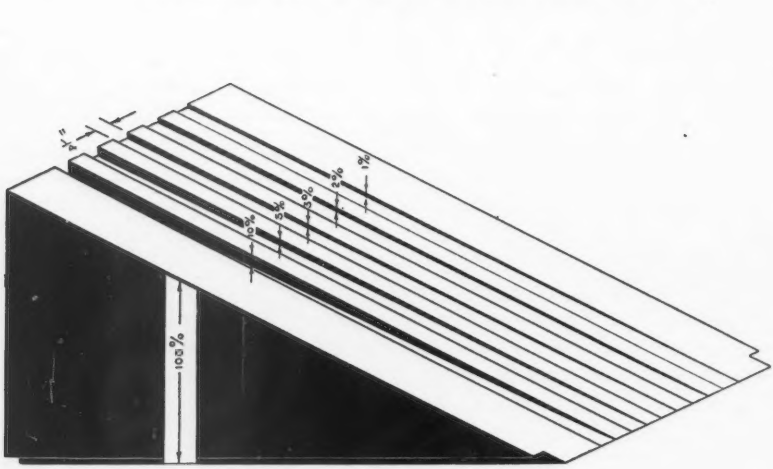

FIG. 3. *Slotted steel wedge penetrameter.*

certain errors related to the shortness of this distance arise. This is illustrated in Fig. 4. The wedge is made so that $EF/FG = PQ/QR$ but on the film the slot PQ' will appear on the wedge of thickness $Q'R'$ and $\frac{PQ'}{Q'R'} \neq \frac{PQ}{QR}$.

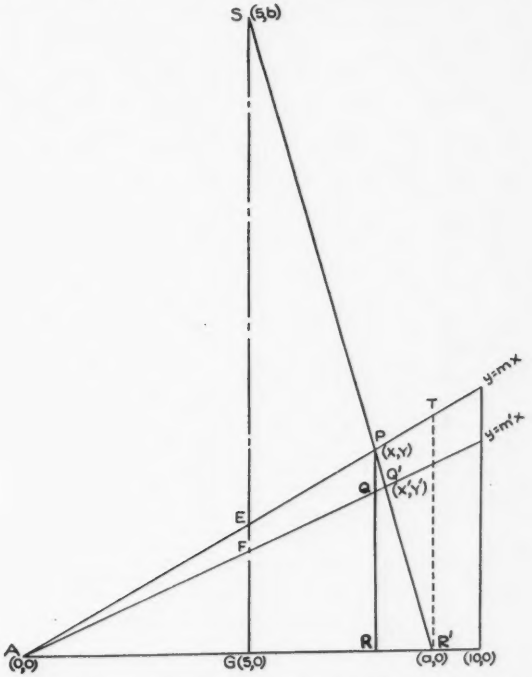

FIG. 4. *Diagram of steel penetrameter showing how distortion arises when short source to film distances are used.*

Hence for points along the film from A to R the effective percentage depth of the slot changes. Another error arises from the fact that the points along the film from A to R do not all receive the same exposure factor, since they are different distances from S. Corrections for these errors can be made easily.

In Fig. 5, the penetrameter sensitivity for "No Screen" film with 0.015 in. lead front screen and 0.030 in. lead back screen are shown both for the original measurements (solid lines) and when all corrections are made (dotted curves). The difference between these sets of curves is smaller than the probable error of the measurements so that for the other films no corrections of this kind were carried out. From Fig. 5 we see that under the ideal conditions obtainable with the penetrameter, the 1% slot was not visible but that the 2% slot was visible in steel of thickness greater than 0.6 in. For 1.0 in. the exposure

factor must lie between 100 and 300 in order to detect a 2% flaw. For 2.0 in. of steel the exposure factor should be somewhere in the range of 200 to 650. If a casting consisted of two thicknesses of 3.0 and 1.0 in. two exposures of

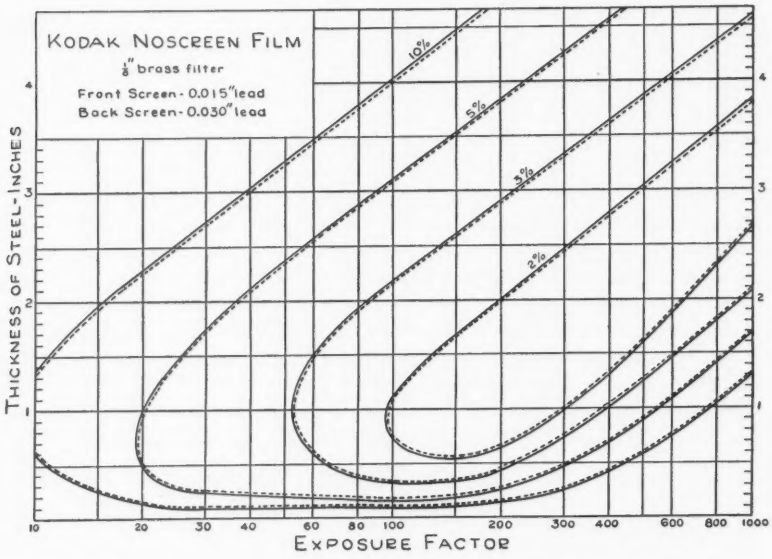

FIG. 5. *Penetrameter sensitivity curves for Kodak "No Screen" film. Solid lines were uncorrected for distortion, while dotted lines show the results after all corrections are carried out. Front screen, 0.015 in. lead; back screen, 0.030 in. lead. Standard development. The percentages marked on the graph give the percentage thickness of the slot in the wedge penetrameter which can just be detected.*

the casting would be required if one used "No Screen" film and a 0.015 in. lead front screen. From Fig. 5 we see that exposure factors of 200 and 600 would be satisfactory*.

The effectiveness of the lead front screen in determining the penetrameter sensitivity is illustrated in Figs. 6, 7, and 8 where results similar to Fig. 5 are shown but with lead front screens of thickness 0.000, 0.030, and 0.060 in. It will be seen that the area enclosed within the 2% sensitivity curve is greatest for 0.030 in. of lead front screen, and smallest for no lead front screen. For most purposes then, a 0.030 in. lead front screen is the most useful for "No Screen" film. For no lead front screen (Fig. 6) the area enclosed by the 2% curve is quite small showing that such a sensitivity can be only just obtained. When a thick lead front screen is used, scattered radiation from the casting

* *The width of the 2% area of course determines the allowable latitude in the exposure factor for a given thickness of casting. The height of the 2% area determines the range of casting thickness which may be examined with one exposure.*

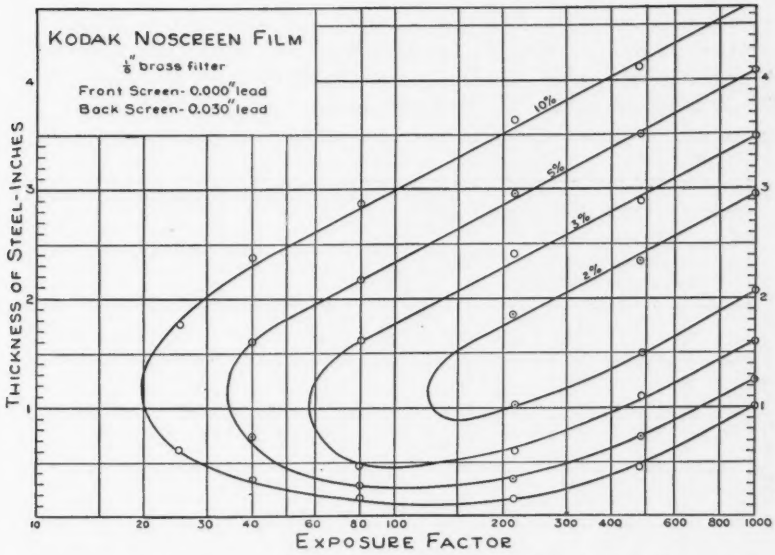

FIG. 6. *Penetrameter sensitivity curves for Kodak "No Screen" film. Front screen, 0.000 in. lead; back screen, 0.030 in. lead. Standard development.*

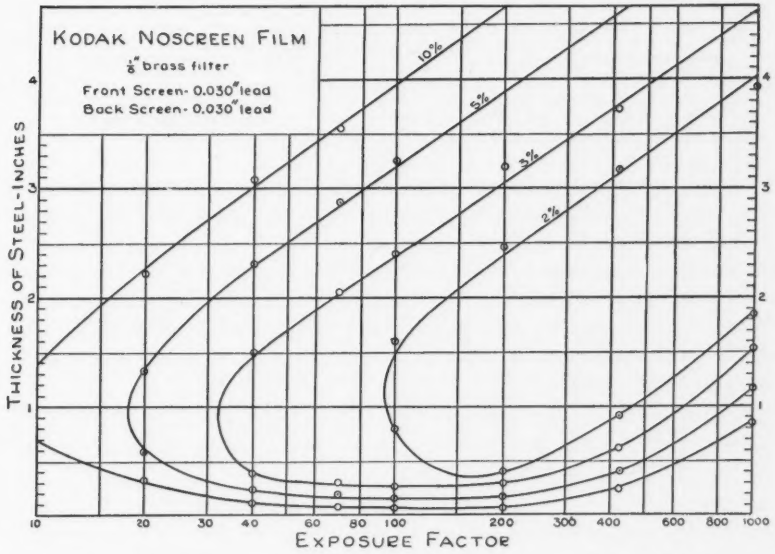

FIG. 7. *Penetrameter sensitivity curves for Kodak "No Screen" film. Front screen, 0.030 in. lead; back screen, 0.030 in. lead. Standard development.*

is more severely cut down so that the sensitivity which can be obtained is increased. However, when the thickness of the lead front screen is increased beyond a certain value, the penetrameter sensitivity obtainable decreases. This is illustrated in Fig. 8. Beyond a certain value the lead front screen serves only to absorb the primary beam without introducing much extra

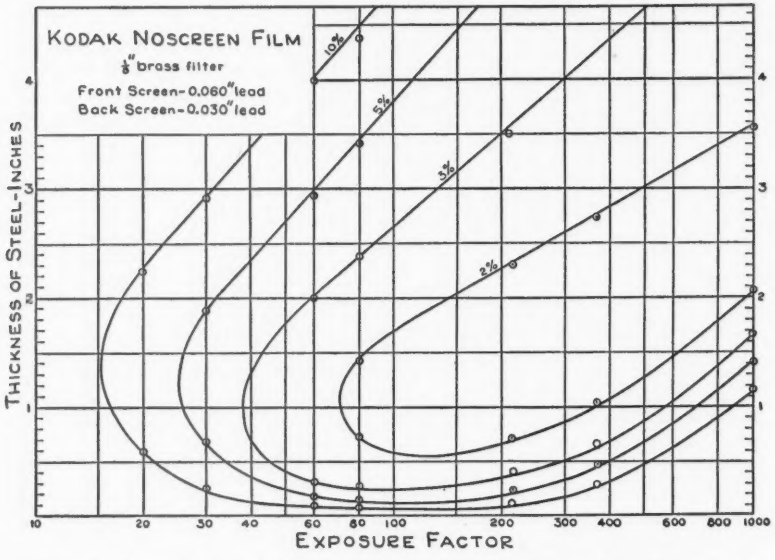

FIG. 8. *Penetrameter sensitivity curves for Kodak "No Screen" film. Front screen, 0.060 in. lead; back screen, 0.030 in. lead. Standard development.*

discrimination against the scattered radiation. Fig. 7 illustrates the fact that a 2% sensitivity can be obtained in a 0.5 in. steel block at exposure factor from 130 to 250 when 0.030 in. lead front screen is used. From Fig. 2 we saw that maximum intensification was achieved in a 0.5 in. steel block using 0.003 in. lead front screen. The great difference between the thickness of lead front screen to produce maximum differential sensitivity and that which gives maximum intensification (i.e., shortest exposure for a given density) is quite apparent.

Similar penetrameter sensitivity curves are shown in Figs. 9 to 14 for Kodak A film, Kodak Blue Brand, Dupont 506, and Ansco Superay A, for a variety of front screen filters. The information presented in Figs. 5 to 14 is summarized in Table I, in which is shown the thickness range of steel which can be radiographed, using radium, to give a 2% sensitivity and the exposure factor required for this sensitivity for five varieties of film and for different thicknesses of lead front screen.

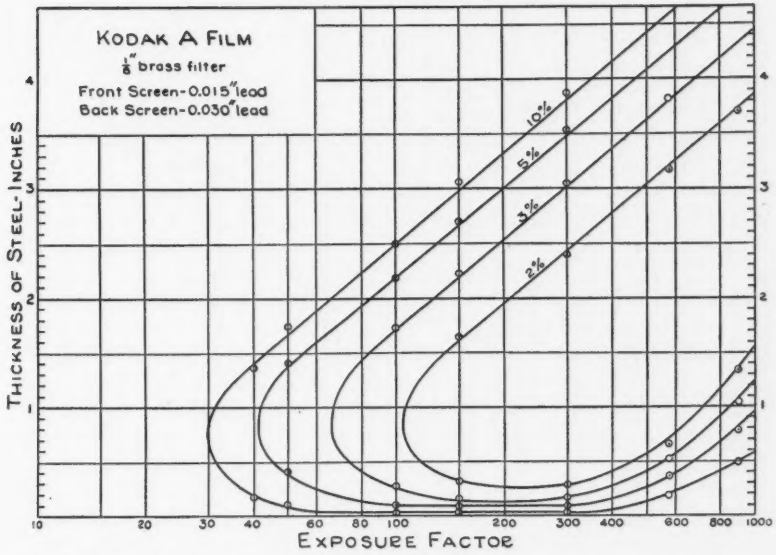

FIG. 9. *Penetrameter sensitivity curves for Kodak A film. Front screen, 0.015 in. lead; back screen, 0.030 in. lead. Standard development.*

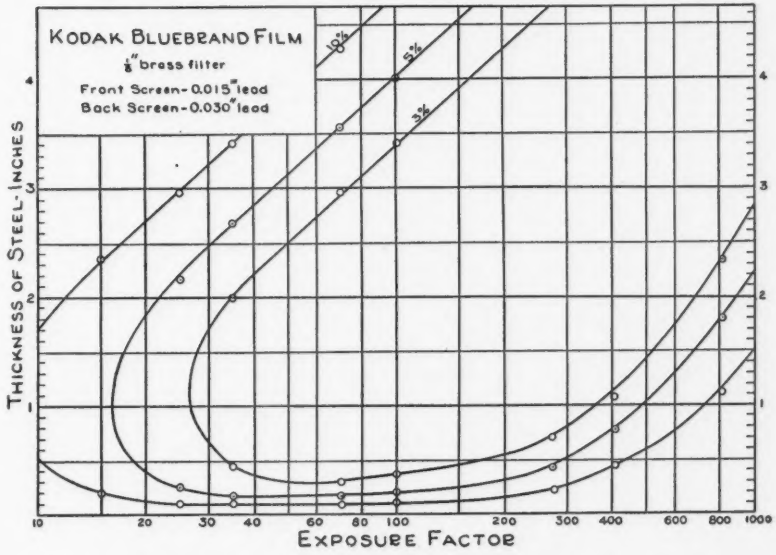

FIG. 10. *Penetrameter sensitivity curves for Kodak Blue Brand film. Front screen, 0.015 in. lead; back screen, 0.030 in. lead. Standard development.*

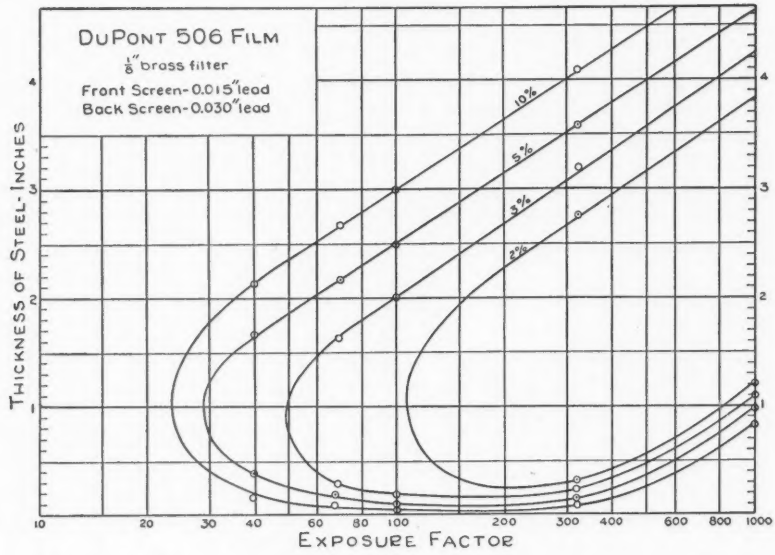

FIG. 11. *Penetrameter sensitivity curves for Dupont 506 film. Front screen, 0.015 in. lead; back screen, 0.030 in. lead. Standard development.*

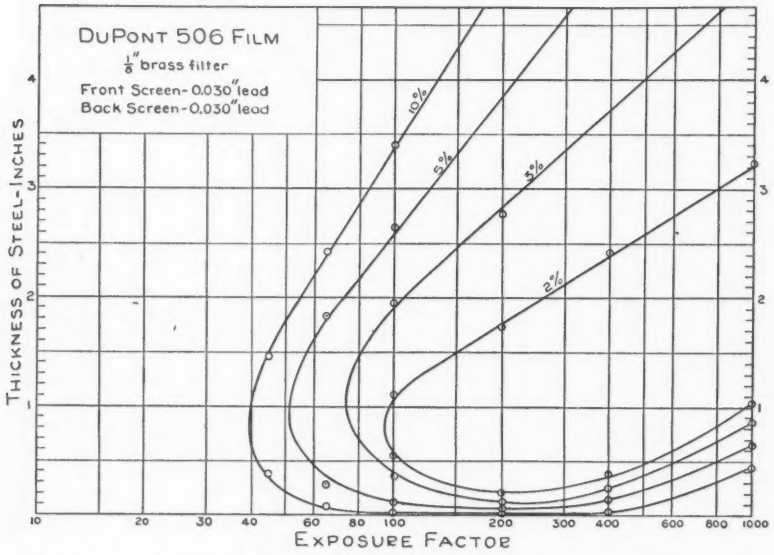

FIG. 12. *Penetrameter sensitivity curves for Dupont 506 film. Front screen, 0.030 in. lead; back screen, 0.030 in. lead. Standard development.*

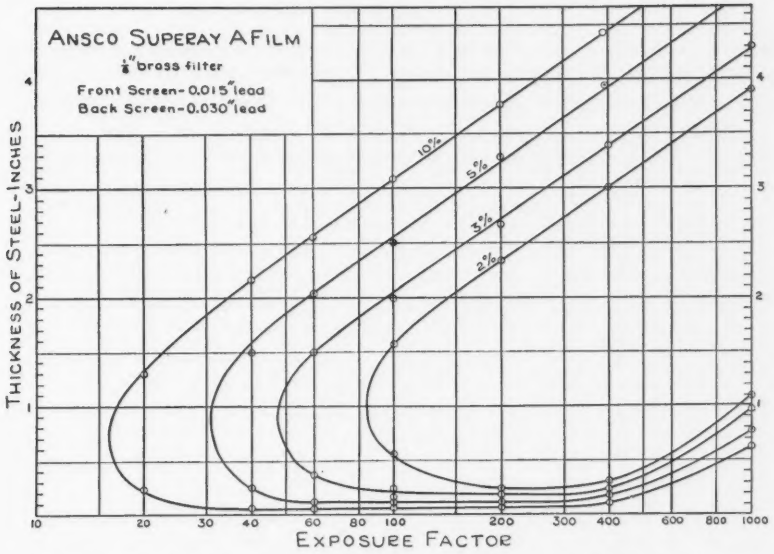

FIG. 13. *Penetrameter sensitivity curves for Ansco Superay A film. Front screen, 0.015 in. lead; back screen, 0.030 in. lead. Standard development.*

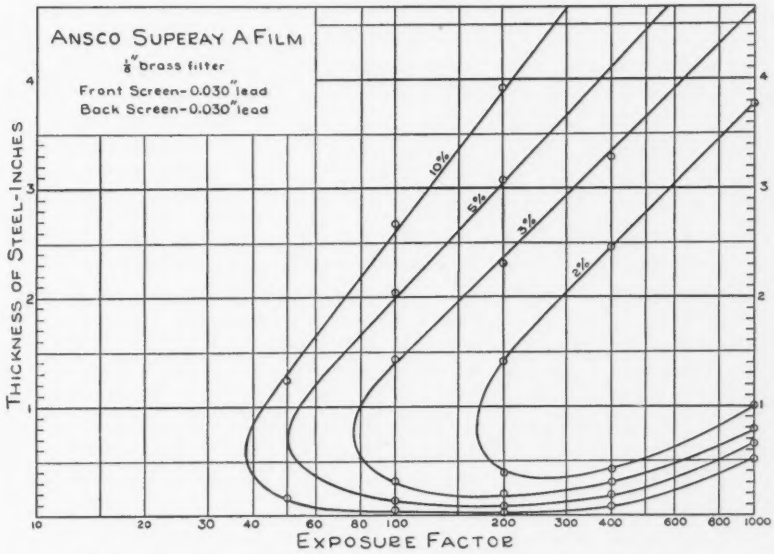

FIG. 14. *Penetrameter sensitivity curves for Ansco Superay A film. Front screen, 0.030 in. lead; back screen, 0.030 in. lead. Standard development.*

TABLE I

SUMMARY OF RANGES OF THICKNESS OF STEEL IN WHICH A 2% FLAW MAY BE DETECTED FOR DIFFERENT EXPOSURE FACTORS, TYPES OF FILM, AND THICKNESSES OF LEAD FRONT SCREENS

Film	Lead front screen, in.	Exposure factor, mgm. × min./in.²					
		80	100	150	200	400	1000
		Range of thickness of steel in which 2% flaw may be detected, in.					
Kodak "No Screen" Film	0.000			0.9 to 1.5	1.0 to 1.75	1.3 to 2.3	2.1 to 2.9
	0.015		0.75 to 1.1	0.6 to 1.6	0.7 to 2.0	1.3 to 2.75	2.7 to 3.8
	0.30		0.8 to 1.5	0.4 to 2.1	0.4 to 2.4	0.9 to 3.1	1.9 to 4.0
	0.043	1.1 to 1.6	0.8 to 1.9	0.6 to 2.2	0.6 to 2.4	0.9 to 2.7	1.8 to 3.5
	0.060	0.75 to 1.4	0.6 to 1.7	0.6 to 2.0	0.65 to 2.3	1.1 to 2.8	2.1 to 3.6
Kodak A	0.015			0.3 to 1.6	0.25 to 1.9	0.4 to 2.75	1.6 to 3.8
Kodak Blue Brand			2% not observable				
Dupont 506	0.000					0.7 to 1.7	1.3 to 2.8
	0.015			0.3 to 1.9	0.25 to 2.25	0.4 to 2.9	1.2 to 3.8
	0.030		0.6 to 1.1	0.3 to 1.5	0.25 to 1.75	0.4 to 2.3	1.1 to 3.2
Ansco Superay A	0.000					0.7 to 1.9	1.2 to 2.7
	0.015		0.5 to 1.6	0.3 to 2.1	0.25 to 2.3	0.3 to 3.0	1.1 to 3.9
	0.030				0.4 to 1.4	0.4 to 2.4	1.0 to 3.8

Discussion

Table I and Figs. 5 to 8 indicate that when "No Screen" film is used a lead front screen 0.030 in. thick will in general enable one to "examine" with a 2% technique the maximum thickness range of casting. The exposure factor required is 100 or greater. In general, thicker or thinner front screens will reduce slightly the range of thickness in which a 2% sensitivity may be obtained. However for a limited range of thicknesses a thicker lead front screen (0.043 in. or 0.060 in.) can yield a 2% sensitivity at exposure factor 80.

Table I and Figs. 9, 11, and 13 indicate that for most purposes Dupont 506 and Ansco Superay A should be used with 0.015 in. lead front screens. For a given exposure factor the range of thicknesses which may be radiographed to give a 2% sensitivity is slightly greater for Ansco Superay A than for Dupont 506, Kodak A, or "No Screen" film although the differences are very slight. Sections of steel thinner than 0.50 in. can hardly be radiographed to give a 2% sensitivity using "No Screen" film. Steel in thicknesses down to 0.30 in. can be radiographed with a 2% technique about equally well at exposure factor 150 for either Kodak A, Dupont 506, or Ansco Superay A film. These results are in general agreement with those of Nodwell and Morrison (2).

It is impossible to include in this paper results such as these for all films but it is felt that in a place where many castings are being radiographed, penetrameter sensitivity curves of this type should be constructed by the use of a

wedge penetrameter and that exposures of castings should be planned on the basis of such information rather than from graphs relating density to exposure factor. It should be realized that in many cases the sensitivity indicated in Figs. 6 to 14 cannot be achieved owing to scattered radiation from a complicated casting, but such curves do enable one to plan the exposure technique for any casting quickly and with greater accuracy than is possible by other methods.

Acknowledgments

The authors wish to express their appreciation to the National Research Council of Canada for their financial support in this project and especially to Mr. A. Morrison of the Radiology Division of the National Research Council for his part in initiating this work and for his many helpful suggestions. Acknowledgments are due Prof. E. L. Harrington, Head of the Department of Physics of the University of Saskatchewan, for his continued support of the project and to Mr. A. H. Cox of the Instrument Shop, for his technical assistance.

References

1. LAURENCE, G. C., BALL, L. W., and ARCHIBALD, W. J. National Research Council of Canada Bulletin. 1942.
2. NODWELL, E. M. and MORRISON, A. National Research Council of Canada Bulletin No. 1134. July, 1943. *Also in* A.S.T.M. Bulletin, p. 25. March, 1944.

ABSORPTION MEASUREMENTS OF SOUND IN SEA WATER[1]

By G. J. Thiessen, J. R. Leslie[2], and F. W. Simpson

Abstract

Sound absorption measurements, made with a diverging beam in sea water, are given. They cover frequencies from 0.35 to 2.3 Mc. per second and are somewhat lower than those given by Richardson for fresh water. Conclusive comparison between these results and fresh water results cannot be made. Advantages of using long distances are discussed.

Introduction

Owing to the use of sound in underwater signalling and submarine detection, the war was responsible for a considerable revival of interest in the absorption of sound in water, particularly in the ultrasonic region. A number of investigators had already published results in the literature which seemed to indicate a large absorption band in the frequency region of 1 Mc. per sec. and lower. But variations by factors as large as 10 were fairly common, depending on the details of the particular experimental methods used. Thus at a frequency of 1 Mc. per sec., Sörensen (17) gets an amplitude absorption coefficient α of 0.0057 cm.$^{-1}$, Hartmann and Focke (8) get 0.014 cm.$^{-1}$, whereas Richardson's (16) value is 0.00045 cm.$^{-1}$ For comparison purposes, as many data as could be obtained to date are plotted in Fig. 2, where the amplitude absorption coefficient α and the attenuation in decibels per meter are plotted against the frequency. All results except the present are for fresh water.

Since the measurements were not all made at the same temperature they are reduced, wherever possible, to 20° C. and to this end the classical variation with temperature was used. From Stokes' well known formula the amplitude absorption coefficient α is given by

$$\alpha = \frac{8\pi^2 f^2 \eta}{3\rho v^3}$$

where f is frequency, η is viscosity, ρ the density, and v the velocity of sound in the medium. Hence the temperature variation will depend on η, v, and ρ. Using the values for η and ρ from the International Critical Tables and the values for v from references (13) and (19), the results for $\frac{\alpha}{f^2}$ are plotted in Fig. 1. For comparison purposes some experimental values from the literature are also shown in arbitrary units. The check is as close as the spread among experimenters' values, and thus justifies the use of the curve for reduction of values to the same temperature.

[1] *Manuscript received in original form January 20, 1948, and, as revised, May 5, 1948. Contribution from the Physics Division, National Research Laboratories, Ottawa, Canada. Issued as N.R.C. No. 1795. This work was done during the war at the request of the Director of Scientific Research and Development, Royal Canadian Navy.*

[2] *At present with the Ontario Hydroelectric Power Commission, Toronto.*

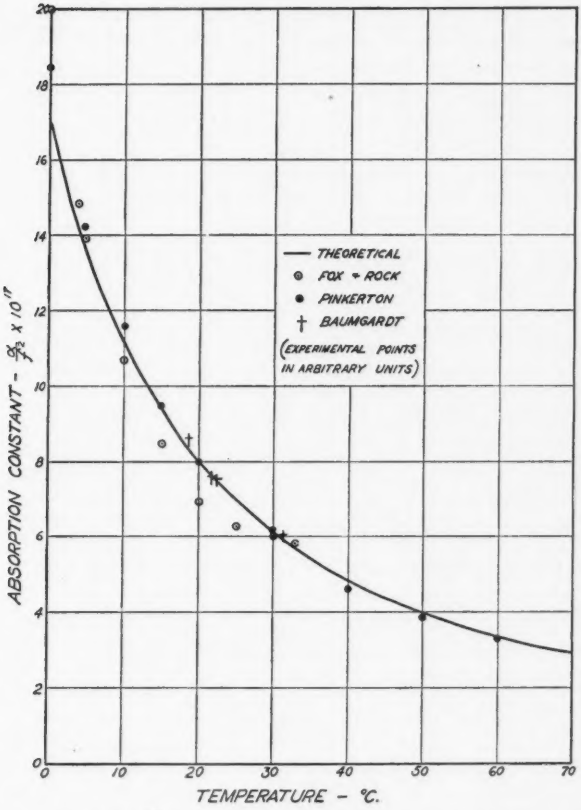

FIG. 1. *The variation of* $\frac{\alpha}{f^2}$ *as a function of temperature. The experimental values are in arbitrary units.*

The reproducibility for different investigators is probably not as poor as Fig. 2 would indicate. For instance, the values of Sörensen's have been definitely proved to be too high owing to radial resonances in the tube (5). Claeys, Errera, and Sack have, in fact, been able to get values even higher than those of Sörensen's by simply decreasing the diameter of the tube containing the water.

The second factor that has given rise to much of the discrepancy among the early results is absorption due to cavitation (15, p. 45). Boyle, Taylor, and Froman (4) have found that cavitation may begin at 0.03 w. per cm.^{2} and experiments on absorption as a function of intensity by Fox and Rock (18) bear this out, showing an increased absorption as the intensity is increased beyond about 0.04 w. per cm.^{2} The high frequency supply used by Hartmann and Focke was capable of an output of 100 w., and, since an efficiency of 10%

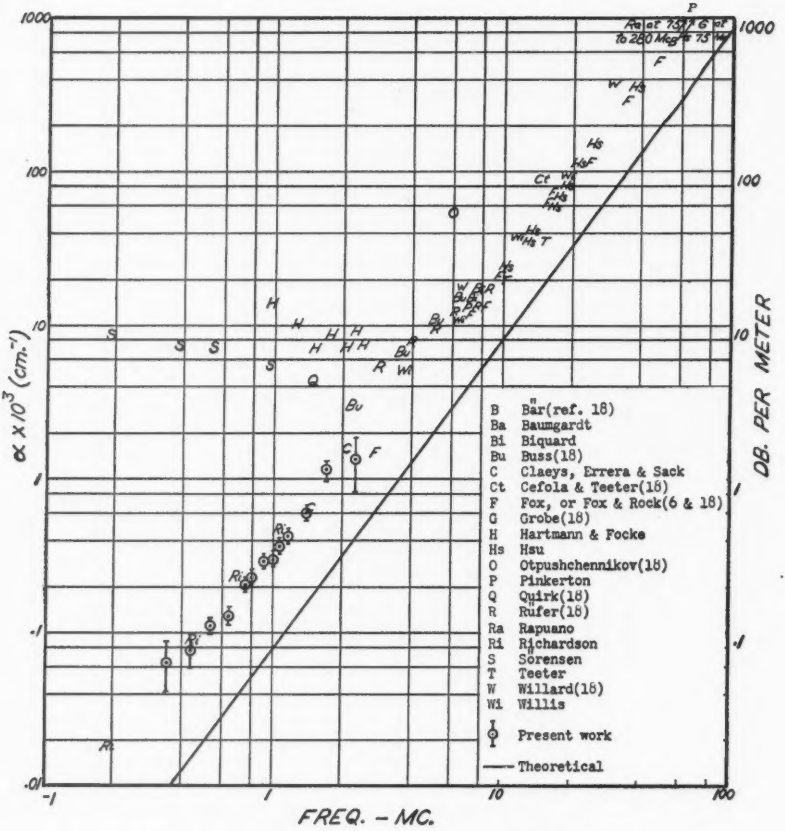

FIG. 2. *The absorption coefficient α (cm.⁻¹) as a function of frequency. The points W-W and P-P should really be joined by a straight line. They were determined by calculation of α for the extreme frequencies from the average* $\frac{\alpha}{f^2}$ *as given by the corresponding authors.*

is easily obtained with quartz at resonance, this would give a possible intensity of 2.5 w. per cm.² for their crystal. This is well in the cavitation region. Richardson, who believes that most radiation pressure methods require too high intensities for reliability, obtained the qualitative result that, whenever intensity was increased to the point of turbulence, the absorption coefficient was increased severalfold.

The remaining points, while suggesting more nearly a straight line, still spread out over a wide range, particularly at the lower frequencies. The following factors have been suggested as possible causes of the scatter as well as of the discrepancy with theory:

(1) Energy is lost from the beam owing to scattering caused by local inhomogeneities of the water (e.g., crystallization). This was suggested by Lucas (11), and Biquard (2) also claims to have found evidence to substantiate this. Richardson and Pinkerton (12), however, have detected no scattered energies, though the latter has some secondary evidence of this in the change of the ratio of α(observed) to α(calculated) at temperatures below 15° C. Since the area over which the scattered radiation is spread is rather large, it is expected that this will be difficult to detect. It is probably worthy of notice that a radiation pressure detector was used by Biquard and since this is nearly nondirectional, it is possible that it may respond to radiation coming directly from the quartz crystal. The complicated directionality pattern of quartz is mentioned below.

(2) The assumption of plane waves is usually made, yet Richardson and Willard (18) have shown that there is an appreciable amount of divergence. Born (3) calls attention to the fact that both divergence and convergence are possible at distances generally used in absorption measurements. Specific corrections for this have been made only by Pinkerton, Willard, and Hsu (14), although some of the irregularities are no doubt smoothed out by the customary use of large detectors (see Fox and Rock, reference (18)).

(3) Another cause of divergence that is less easily corrected for, at short distances, is that due to variations in phase and amplitude across the crystal face. In calculating directionality patterns, it is usually assumed that the amplitude and phase across the face of the transmitting piston are constant. How far from valid this assumption may be is shown by pictures such as given by Hiedemann (reference (9), pages 9 and 11) or by Grobe (reference (7), page 335). Only by going to larger distances is it possible to tell accurately what the intensity changes, due to geometry, will be.

Apparatus and Method

The present work was done in Vancouver harbor where, through the courtesy of the Pacific (Coyle) Navigation Co. Ltd., the use of their dock was obtained. This afforded a stretch of water free from obstacles, for a distance of 30 m., where the depth varied from 4 to 6 m., depending on the tides. The temperature was also dependent on the tides, varying by approximately 1° on either side of 10° C. This variation was not corrected for, since this is beyond the accuracy claimed for the present experiments.

In the transmitter, X-cut rochelle salt was used. Four crystals 1 by $\frac{3}{8}$ by $\frac{1}{4}$ in. had their $\frac{3}{8}$ in. dimension ground down to 3/16 in., and were then connected in series-parallel, so that the $\frac{1}{4}$ by 1 in. faces were the transmitting faces. The crystals were mounted in a circular piece of bakelite, "vulcaloc" being used to stick them into place. The crystal surfaces usually protruded somewhat above the bakelite surface and, when the "vulcaloc" was dry, they were ground down flush with the bakelite. A thin rubber sheet from a

surgeon's rubber glove was then cemented over the whole face, thus effectively waterproofing it without interfering with the cooling effect of the water. The crystal mount was then mounted on one end of a cylindrical brass housing.

The cylindrical, brass, waterproof housing, $3\frac{1}{2}$ in. in diameter, contained two 6L6's connected in parallel, to supply the power to the rochelle salt crystals. They in turn were driven by a 6AG7 tube also contained in the same housing. Resistance plate loads were used throughout but no effort was made to secure a flat frequency response. The power and signal were supplied through cables from above water, a Clough Brengle signal generator being used as a source of the desired frequency.

The receiver was made of a small piece of crystal with dimensions $\frac{1}{4}$ by $\frac{1}{4}$ by 1/16 in., the larger face being the receiving face. This was set in polystyrene and covered with a polystyrene film, and then mounted on the end of a pre-amplifier housing, similar to the transmitter but smaller. The receiver was made small so that it would not have too sharp a directionality pattern and would thus facilitate the search for the center of the sound beam by reducing amplitude variations due to slight changes in orientation.

The preamplifier consisted of two 6AC7's, the first one being used as an amplifier while the second, connected as a cathode-follower, fed a concentric line to the amplifier above. The main amplifier was a superheterodyne all-band receiver with the audio stage removed. The a.v.c. voltage was controlled manually by means of a potentiometer, thus permitting the gain to be changed at will.

The procedure consisted of mounting the transmitter at a depth of about 2 to 3 m., depending on the tides, and sending the beam parallel to the floating dock toward the receiver. The receiver was mounted on the end of a long pole. It was not assumed that the center of the beam was along the line perpendicular to the crystal face, but the procedure involved rather a search for a maximum reading of the detector, as the two co-ordinates perpendicular to the approximate beam direction were varied. The distance between transmitter and detector was varied between 3 to 30 m., and since the sound pressure is given by

$$P_x = \frac{P_o e^{-\alpha x}}{x},$$

pressure measurements at two distances will enable the calculation of the amplitude absorption coefficient α. P_x is the sound pressure at distance x from the receiver. Up to 10 or 11 readings were taken for the same frequency and the error calculated statistically from the fluctuations of these readings about the mean.

Discussion of Results

The comparison of the present salt water results with those for fresh water cannot be made without some justification, and this lies mainly in the contradictory results in the literature. Claeys, Errera, and Sack found a decided

increase of the absorption coefficient with increasing salinity, so that for sea water (which is 3.0% salt, or about 0.5 mole per liter) $\frac{2\alpha}{f^2}$ should be very nearly doubled. Buss (18) on the other hand finds that 6.6% sodium chloride added to water has no appreciable effect on $\frac{2\alpha}{f^2}$ but that higher concentrations will cause a drop in this value. His actual values for $\frac{2\alpha}{f^2}$ seem very high but should still serve to show the effect of salinity. Rüfer (18) checks the values of Buss in an approximate way, also getting a decrease in absorption with increased salinity. However, the effect is so small that a 3.0% solution should not differ by more than 6% from fresh water at any of the frequencies that he used.

Thus, if the results of Buss and Rüfer may be accepted then, to within the accuracy claimed, the present results may be compared directly with fresh water results. If the results of Claeys, Errera, and Sack are given more weight, then the present results can only be considered to give an upper limit and would be approximately twice too high.

The values obtained for α are given in Table I, together with the corresponding statistical errors (calculated from the deviation from the mean). The figures in the fourth column are those for α corrected to 20° C. according to Fig. 1, and are the ones plotted in Fig. 2. The mean value for $\frac{2\alpha}{f^2}$ at 20° C. is about 71, and, if the values for the lowest and highest frequency are neglected owing to the large error, then the average $\frac{2\alpha}{f^2}$ comes to 70.

TABLE I

ABSORPTION COEFFICIENTS FOR VARIOUS FREQUENCIES

f, mc.	Db./m.	$\alpha \times 10^4$, cm.$^{-1}$	$\alpha \times 10^4$ (at 20°C.)	$\frac{2\alpha}{f^2} \times 10^{17}$ (at 20° C.)
0.355	0.080	0.92 ± 0.35	0.66	103
0.450	0.092	1.06 ± 0.18	0.76	74
0.550	0.138	1.59 ± 0.12	1.13	74
0.65	0.161	1.84 ± 0.09	1.31	62
0.75	0.233	2.90 ± 0.09	2.07	67
0.80	0.282	3.24 ± 0.14	2.32	71
0.90	0.350	4.03 ± 0.14	2.88	71
1.00	0.360	4.15 ± 0.28	2.97	60
1.08	0.440	5.10 ± 0.60	3.60	62
1.20	0.520	6.00 ± 0.37	4.30	71
1.45	0.720	8.30 ± 0.37	6.00	83
1.70	1.38	15.9 ± 1.5	11.3	78
2.30	1.61	18.4 ± 5.8	13.1	48

As is seen from the graph, the values check quite closely with the results of Richardson and those of Claeys, Errera, and Sack, who made measurements in this frequency region. Before definite conclusions can be drawn from this, it

will be necessary to repeat these experiments in fresh water, or at least to determine more conclusively the effect of salt on the absorption coefficient of water.

One of the reasons for fluctuations, particularly at low frequencies, was the reflection from the surface and bottom. This in fact set the lower limit to the frequencies that could be used and still result in reasonably consistent readings. The amount of surface reflection was usually judged by the fluctuations in the meter reading caused by waves and ripples when both transmitter and receiver were fixed. Bottom reflections were not, of course, as easily detected. These reflections can be expected to cause considerable trouble below 500 kc. for the water depths used, particularly since it becomes more necessary to get accurate readings owing to the decreasing absorption coefficient.

The high frequency limit was set by the fact that the directionality pattern became very complicated and the main beam might make any angle within 20° or so with the transmitter axis. Large side lobes would appear and show no axial symmetry. This made the hunt for the center of the beam difficult and resulted in the large error shown by the reading at the highest frequency. Furthermore, since the distances at these high frequencies have to be made necessarily shorter to obtain any signal, the correction for the difference in location of the actual source and the effective source (the latter is actually behind the former, see reference (20)) becomes quite important. Since this fact was not taken into account, the values at the highest frequency may be expected to be too low.

It is planned to continue experiments using relatively large distances, in both fresh and salt water.

References

1. BAUMGARDT, E. Compt. rend. 202 : 203. 1936.
2. BIQUARD, P. Compt. rend. 202 : 117. 1936.
3. BORN, H. Z. Physik, 120 : 383. 1943.
4. BOYLE, R. W., TAYLOR, G. B., and FROMAN, D. K. Trans. Roy. Soc. Can. 23 : 187. 1929.
5. CLAEYS, J., ERRERA, J., and SACK, H. Trans. Faraday Soc. 33 : 136. 1937.
6. FOX, F. E., and ROCK, G. D. Phys. Rev. 70 : 68. 1946.
7. GROBE, H. Physik. Z. 39 : 333. 1938.
8. HARTMANN, G. K. and FOCKE A. B. Phys. Rev. 57 : 221. 1940.
9. HIEDEMANN, E. Grundlagen und Ergebnisse der Ultraschallforschung. Walter De Gruyter & Co., Berlin W35. Printed by Metzger and Wittig in Leipzig. Archiv.—Nr. 525739. 1939.
10. HSU, E. T. J. Acoustical Soc. Am. 17 : 127. 1945.
11. LUCAS, R. Compt. rend. 201 : 1172. 1935.
12. PINKERTON, J. M. M. Nature, 160 : 129. 1947.
13. RANDALL, C. R. J. Research Natl. Bur. Standards, 8 : 79. 1932.
14. RAPUANO, R. A. Phys. Rev. 72 : 78. 1947.
15. RICHARDS, W. T. Rev. Modern Phys. 11 : 36. 1939.
16. RICHARDSON, E. G. Proc. Phys. Soc. London, 52 : 480. 1940.
17. SÖRENSEN, C. Ann. Physik, 26 : 121. 1936.
18. TEETER, C. E., JR. J. Acoustical Soc. Am. 18 : 488. 1946. (Other references given here.)
19. WILLARD, G. W. J. Acoustical Soc. Am. 19 : 235. 1947.
20. WILLIAMS, A. O., JR. J. Acoustical Soc. Am. 19 : 156. 1947.
21. WILLIS, F. H. J. Acoustical Soc. Am. 19 : 242. 1947.

THE γ-RAYS OF THORIUM CC′[1]

By S. C. Fultz[2] and G. N. Harding[3]

Abstract

At least two energy level schemes have been proposed for the ThC′ nucleus, which is excited in the β-disintegration ThCC′. That of Ellis (1933) includes three γ-rays of energies 0.726, 1.62, and 1.80 Mev., the 1.62 Mev. ray being doubtful. The level scheme of Latyschev and Kulchitsky (1940) has eight γ-rays including one of energy 2.2 Mev., for which no corresponding long-range α-particle group has been observed. The two level schemes lead to widely differing values for the total γ-ray energy of ThCC′. In the present investigation a value for the total γ-ray energy of ThCC′ has been obtained by measuring coincidences between the γ-rays of ThCC′ and the subsequently emitted α-particles of ThC′. It is shown that this value (0.14 Mev.) favors the level scheme of Ellis, including only the γ-rays of energy 0.726 and 1.80 Mev., and taking the former as electric quadrupole. It was found that under certain conditions the external bremsstrahlung excited by the β-rays of ThCC′ in the source-holder contributed appreciably to the coincidence rate. Precautions were taken to minimize this effect.

Introduction

In the β-disintegration ThC $\rightarrow$ ThC′, the product nucleus may, in a certain fraction of the disintegrations, be left in an excited state. The de-excitation process occurs, according to Gamow (15), in one of two ways. Either the excitation energy is carried off by the α-particles subsequently emitted by ThC′, thus giving rise to a long range group of α-particles; or the nucleus falls to a lower energy level by emission of a γ-ray. A close relationship between energies of γ-rays and energy differences of such groups of α-particles, therefore, would be expected.

Accurate measurements of the energies of ThC′ α-particles were first made by Rosenblum and Valadares (25), who observed four groups corresponding to disintegration energies of 10.72, 9.78, 9.63, and 8.94 Mev. From the energy levels giving rise to these groups we might expect γ-rays of energies 1.78, 1.09, 0.94, 0.84, 0.69, and 0.15 Mev. originating from ThCC′. Further measurements were made by Rutherford, Wynn-Williams, Lewis and Bowden (27), and later by Lewis and Bowden (23), using improved techniques. The latter authors were able to detect only α-particle groups corresponding to disintegration energies of 10.744, 9.673, and 8·947 Mev., suggesting γ-rays of energies 1.797, 1.071, and 0.726 Mev.

Some measurements have also been made on the γ-rays of ThCC′. Ellis (12, 13), using a semicircular focusing magnetic spectrograph, examined the internal conversion electrons of thorium active deposit (ThB + C + C′ + C″). Among the γ-rays which he identified were three which he attributed to ThCC′. These are of quantum energies 1.802, 1.623, and 0.726 Mev., of

[1] *Manuscript received April 30, 1948.*

Contribution from the Division of Atomic Energy, Chalk River Laboratory, National Research Council of Canada. Issued as N.R.C. No. 1804.

[2] *Now at McGill University.*

[3] *Present address: Atomic Energy Research Establishment, Harwell, England.*

which the first and last are in agreement with the measurements of Lewis and Bowden. The energy level scheme proposed by Ellis on the basis of these measurements is shown in Fig. 1, (*a*).

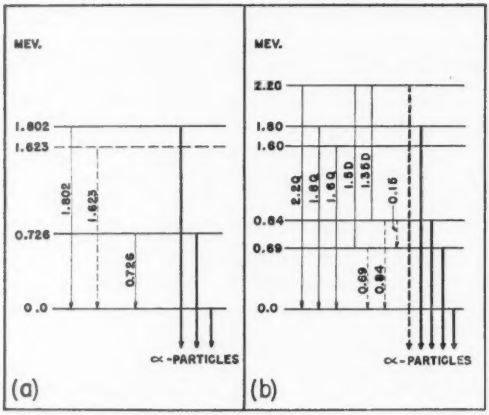

FIG. 1. *Energy levels of ThC′ nucleus proposed by (a) Ellis and (b) Latyschev and Kulchitsky. Heavy lines denote α-particles, fine lines γ-rays.*

Alichanov and Dzelepov (1) examined the positron spectrum of thorium active deposit, using a semicircular focusing magnetic spectrometer, with two Geiger-Müller counters in coincidence. They identified hard γ-rays of energies 2.20, 1.80, 1.60, 1.50, and 1.35 Mev., which they attributed to the transition ThCC′. Measurements by Latyschev and Kulchitsky (22) on the recoil electron spectrum due to the γ-rays from thorium active deposit confirmed the measurements of Alichanov and Dzelepov on the energies of these hard γ-rays. The two sets of results from the Russian workers establish the multipolarities and intensities of these radiations. The error in the intensity measurements was estimated to be from 5 to 10%.

Of particular importance is the fact that these workers observed a 2.2 Mev. γ-ray which they attributed to ThCC′. If such an excitation level is present, one would expect to find a long range group of α-particles, corresponding to a disintegration energy of 11.15 Mev. Since the probability of emission of a long range α-particle increases more rapidly with excitation energy than the probability of the alternative process of γ-ray emission, this group of α-particles should be easily detectable, whereas Rutherford, Wynn-Williams, and Lewis (26) found, in a special search for α-particles of energy greater than 10.7 Mev., none having an intensity greater than 1/10,000 of the 10.7 Mev. group. A level scheme for ThC′ proposed by Latyschev and Kulchitsky is shown in Fig. 1, (*b*).

In order to obtain further data on this problem, the authors undertook the measurement of the total γ-ray energy emitted per disintegration of ThCC′.

The total γ-ray energy expected, according to the two level schemes, will be the sum of contributions from all the γ-rays which are given in each of Tables I and II. The intensities of the hard radiations are those given by the

TABLE I

HARD* γ-RAYS OF THCC′ AS SUGGESTED BY LATYSCHEV AND KULCHITSKY (22)

γ-ray energy, Q, Mev.	Intensity, p	Multipolarity	Energy per disintegration, $p \cdot Q$, Mev.
2.20	0.027	Dipole	0.060
1.80	0.033	Quadrupole	0.060
1.60	0.054	Quadrupole	0.086
1.50	0.020	Dipole	0.030
1.35	0.019	Dipole	0.026

** In addition, there would be contributions from low energy γ-rays. As there has been no certain identification of low energy γ-rays arising from ThCC′, only the contribution of the 0.726 Mev. γ-ray (see Table II) will be added in evaluating the total γ-ray energy.*

TABLE II

γ-RAYS OF THCC′ AS SUGGESTED BY C. D. ELLIS (12, 13)

γ-ray energy, Q, Mev.	Intensity, p	Multipolarity	Energy per disintegration, $p \cdot Q$, Mev.
1.80	0.033	Quadrupole	0.060
1.62	0.054	Quadrupole	0.088
0.726	0.110	Quadrupole	0.080
	0.339	Dipole	0.246

Russian workers. For the 0.726 Mev. radiation, the intensity is calculated from the measurements of Flammersfeld (14) using the theoretical internal conversion coefficients of Hulme (19) and Taylor and Mott (33). Intensity values are given in quanta per disintegration of ThC′.

A recent measurement by Johansson (20), who found the intensity of the 0.726 Mev. γ-ray to be 0.2 quanta per disintegration ThCC′, does not enable us to decide between the electric dipole and quadrupole values but is sufficient to rule out the possibility of this ray being magnetic dipole, in which case the intensity would be much lower.

The various possible values for the total γ-ray energy per disintegration according to the above level schemes are summarized in Table III. Since the multipolarity of the 0.726 Mev. γ-ray is uncertain, the values in Table III

have been calculated for two possibilities, electric dipole and electric quadrupole. In the last row of Table III the total γ-ray energy has been evaluated on the basis of Ellis's level scheme, but omitting the contribution from the 1.62 Mev. γ-ray, the origin of which has not been established (13).

TABLE III

POSSIBLE VALUES FOR TOTAL γ-RAY ENERGY OF THCC′

Level scheme according to:	Total γ-ray energy in Mev. if 0.726 Mev. ray is:	
	Dipole	Quadrupole
Latyschev and Kulchitsky	0.508	0.342
Ellis	0.394	0.228
Ellis (excluding 1.62 Mev. radiation)	0.306	0.140

Experimental Method

The total γ-ray energy was determined by observing coincidences between the γ-rays of ThCC′ and the α-particles of ThC′D which are subsequently emitted with a half-period of about 0.3 μsec. (6). In order to ensure that no coincidences were lost in the interval between emission of γ-ray and α-particle, it was necessary to make the resolving time of the coincidence mixer greater than this interval. The resolving time was therefore varied between 0.6 and 4 μsec., and only those results used which lay on the flat portion of the curve of efficiency vs. resolving time (see Fig. 4). The source used was thorium active deposit, and the α-particles of ThCC″ were removed by absorption.

Under these conditions, the α-particle counting rate is given by (10)

$$q_\alpha = 0.65\, N\, \epsilon_\alpha\,, \tag{1}$$

where N is the number of disintegrations of ThC in unit time, 0.65 is the fraction of this number disintegrating to produce ThC′, and ϵ_α is the efficiency of the α-counter. The counting rate for the γ-counter is given by

$$q_\gamma = 0.65\, N \sum_i \epsilon_{\gamma i} \cdot p_i + 0.65\, N \sum_j \epsilon_{Bj} \cdot p_j + S\,, \tag{2}$$

where p_i and $\epsilon_{\gamma i}$ are respectively the intensity and the efficiency of the γ-counter for a γ-ray i; p_j and ϵ_{Bj} are the corresponding quantities for a bremsstrahlung quantum j; and S is the counting rate due to γ-rays other than those of ThCC′. The bremsstrahlung will be discussed subsequently.

The total coincidence rate, which includes coincidences between ThC′D α-particles and ThCC′ γ-rays, plus those between ThC′D α-particles and bremsstrahlung arising from ThCC′ β-rays, is given by

$$q_c = 0.65\, N\, \epsilon_\alpha \left(\sum_i \epsilon_{\gamma i} \cdot p_i + \sum_j \epsilon_{Bj} \cdot p_j\right) + 2\tau q_\alpha q_\gamma\,, \tag{3}$$

where τ is the resolving time of the coincidence mixer, and the last term on the right hand side is due to random coincidences. Dividing Equation (3) by Equation (1) yields the relation

$$\frac{q_c - 2\tau q_\alpha q_\gamma}{q_\alpha} = \sum_i \epsilon_{\gamma i} \cdot p_i + \sum_j \epsilon_{Bj} \cdot p_j \,. \tag{4}$$

The right hand side of Equation (4) gives the total efficiency of the γ-counter for all γ-rays and bremsstrahlung in coincidence with the α-particles of ThC'D.

For a given geometry, the efficiency of a thick-walled brass γ-counter is proportional (within about 6%) to the quantum energy of the incident radiation, particularly in the region of interest for this work, i.e., 0.5 to 2.6 Mev. (9, 10, 37). Considering a γ-ray of unit intensity, we have

$$Q_i = K\,\epsilon_{\gamma i} \,, \tag{5a}$$

where Q_i is the quantum energy of an incident γ-ray i, and K is a constant. When the radiation consists of several components of different intensities p, this becomes

$$\sum_i p_i\, Q_i = K \sum_i p_i \cdot \epsilon_{\gamma i} \,. \tag{5b}$$

Putting $p_i Q_i = E_i$, where E_i is the total γ-energy of a ThCC' γ-ray per disintegration ThCC', and using Equation (4), we get the simple expression

$$E_1 + E_2 + E_3 + \ldots = K \cdot \frac{q_c - 2\tau q_\alpha q_\gamma}{q_\alpha} - B \,, \tag{6}$$

where B represents the correction due to bremsstrahlung.

$$\text{or} \qquad E_1 + E_2 + E_3 + \ldots = K \cdot \bar{\epsilon}_\gamma - B \,, \tag{7}$$

where $\bar{\epsilon}_\gamma$ denotes the total efficiency of the γ-counter for the ThCC' γ-rays. K can be determined by calibration with sources of known γ-energy, and the remaining quantities on the right hand side of Equation (6) are measurable. Thus the total energy of these rays $E_1 + E_2 + E_3 + \ldots$, can be determined.

Apparatus

The α-particles were counted with a proportional counter constructed of brass tubing and filled with argon, having a central mica window 2.72 mgm. per sq. cm. thick. To absorb the α-particles of ThCC'', a screen of aluminum of thickness 7.01 mgm. per sq. cm. was placed between the source and the window, giving a total of 9.73 mgm. per sq. cm. The pulses were amplified by a high-gain broad-band amplifier before passing to the coincidence mixer. γ-rays were detected by a Geiger-Müller counter of conventional design constructed of brass tubing of wall thickness 1/16 in. and filled with a mixture of argon and ethyl alcohol. A two stage amplifier was used to amplify the pulses before passing to the coincidence mixer, which contained the usual Rossi circuit. Scales of 128 were used to record the total

number of α-counts, γ-counts, and coincidence counts over periods ranging from 4 to 15 hr., from which counting rates were calculated, corrections being made for decay of the source.

Sources of thorium active deposit were prepared by deposition on one side only of small pieces of platinum (0.10 gm. per sq. cm.) and aluminum (0.17 gm. per sq. cm.) foil, in a vessel containing an emanating preparation of radiothorium. The foils were mounted at a fixed distance of 2 cm. from the γ-counter, with the active surface close to the window of the α-counter. In Fig. 2 is shown the geometrical arrangement of the counters.

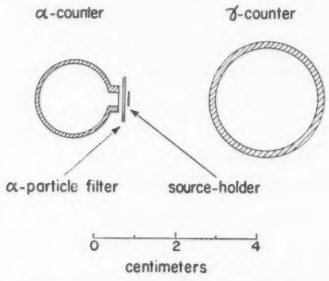

FIG. 2. *Arrangement of the counters.*

CALIBRATION OF THE γ-COUNTER WITH A Co^{60} SOURCE

The γ-counter was calibrated by measuring its efficiency for γ-rays from a Co^{60} source, keeping the geometrical conditions the same as before. Coincidences were observed between the β-rays and γ-rays of Co^{60}, the β-rays being detected in a thin-walled Geiger counter. The efficiency of the γ-counter was then determined by dividing the coincidence counting rate (corrected for random coincidences and cosmic ray background) by the β-ray counting rate. Co^{60} is known to emit one β-ray and two γ-rays of average energy 1.20 Mev. per disintegration (8).

It was considered that a spurious increase in the coincidence rate might arise if a γ-quantum were to be scattered in the wall or window of the β-counter so that the recoil electron entered the β-counter while the scattered γ-quantum actuated the γ-counter. A simple calculation showed that if such an effect were present, the ratio of the β-γ to γ-γ coincidence rates for the Co^{60} source would be less than 2. This ratio was measured in a separate experiment, and no change was observed when absorbers were placed to prevent scattered γ-quanta from the β-counter actuating the γ-counter. It was therefore concluded that no appreciable error in calibration could have been caused by such a process.

The possibility of obtaining coincidence counts between γ-rays and the X-rays caused by absorption of the β-rays was also considered. Calculations showed that this would have negligible effect on the measurements.

The mean value obtained from 10 measurements of the efficiency of the γ-counter for the γ-rays of Co^{60} was $(1.54 \pm 0.02) \times 10^{-3}$. Since there are two γ-rays per disintegration, of mean energy 1.20 Mev., this gives for K (Equation 7) the value $K = (1.56 \pm 0.02) \times 10^{3}$.

Calibration of the γ-counter with a Thorium Active Deposit Source

An independent calibration of the γ-counter was obtained by measuring the counting rate, with the same geometry as before, due to γ-rays from a thorium active deposit source of known strength. The leakage rate in an ion chamber due to the γ-rays from this source was compared with that due to a radium standard; the source strength was calculated from these data, using the value found by Shenstone and Schlundt (28) for the relative strengths of ThC and Ra sources of equal γ-ray activity. The γ-rays of ThB were removed by filtration through lead.

Since the Ra standard was about 100 times stronger than the thorium active deposit, an ion chamber was used with the thorium active deposit which was about 10 times more sensitive than that used with the radium. The sensitivities of the chambers were compared later. Both chambers were constructed of aluminum; one was filled with argon and the other with hydrogen, both to a pressure of 20 atm. The leakage rates were measured with quartz fiber electrometers.

The results of three sets of measurements are given in Table IV.

TABLE IV

Calibration of γ-counter with thorium active deposit source

Trial No.	Source strength, disint. of ThB per sec.	γ-counting rate, counts per min.	γ-counter efficiency × 10^4
1	3.02×10^5	1.714×10^4	9.37 ± 1.1
2	4.82×10^5	2.764×10^4	9.56 ± 0.9
3	3.81×10^5	1.843×10^4	8.1 ± 1.2
Mean			9.0 ± 0.6

The total γ-ray energy of thorium active deposit has been measured by L. H. Gray (17) who found the value 1.44 Mev. per disintegration of ThC. Using this figure, together with the efficiency quoted above, gives a value for the calibration constant $K = (1.60 \pm 0.11) \times 10^{3}$. This value agrees within the experimental error with that of $(1.56 \pm 0.02) \times 10^{3}$ obtained using a Co^{60} source.

The weighted mean of the two values is

$$K = (1.57 \pm 0.02) \times 10^{3}\,.$$

Corrections for Bremsstrahlung

At the outset of this investigation, the very low result ultimately obtained for the total γ-ray energy of ThCC′ was not foreseen, and hence it was not expected that corrections for bremsstrahlung arising from absorption of ThCC′ β-rays in the source-holder would be important. The source-holders were therefore chosen without consideration of the maximum range of the electrons. In view of the low result, however, it later appeared necessary to estimate the magnitude of this effect, and subsequently to adjust the experimental conditions in order to reduce it to a minimum. Both inner and outer bremsstrahlung have to be considered.

The phenomenon of inner bremsstrahlung has been investigated theoretically by Knipp and Uhlenbeck (21) and experimentally by other workers (29, 31, 36). The results of Knipp and Uhlenbeck were used to calculate the inner bremsstrahlung of ThCC′. The effect on the results will be small. The value obtained in the calculation will indicate only the correct order of magnitude, since the calculation makes use of the Born approximation, which holds good only if $\frac{2\pi Ze^2}{hc} \ll 1$, whereas for ThC, $\frac{2\pi Ze^2}{hc} = 0.606$. In Fig. 3, the

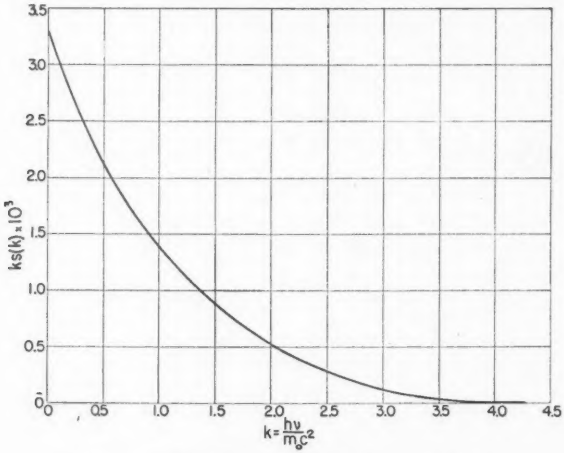

FIG. 3. *Inner bremsstrahlung in the transition ThCC′.*

total energy of radiation having quantum energy between k and $k+dk$, where $k = \frac{h\nu}{m_0c^2}$, is plotted as a function of k. $S(k)$ is the total probability that a light quantum will be emitted in the energy range between k and $k+dk$, and is obtained by summing over all possible energies for the electron.

$$S(k) = \int_{1+k}^{W_0} dW_e \, p(W_e) \, \phi(W_e k) \, , \qquad (8)$$

where $p\,(W_e)$ is the probability of obtaining a disintegration electron of energy W_e, $\phi\,(W_e k)$ denotes the probability per unit energy range of electrons for production of radiation of quantum energy k, and W_0 is the maximum energy of the β-spectrum (including the rest mass m_0 of an electron). The β-ray distribution used in these calculations was that of Richardson and Leigh-Smith (24), which is discussed below. On numerically integrating the curve of Fig. 3, the value obtained for the total energy of the inner bremsstrahlung was found to be 1.76 kev. per disintegration of ThCC′. This is clearly negligible.

The outer bremsstrahlung arises from absorption of the energy of the β-rays by external atoms and is a mode of energy dissipation alternative to ionization by collision. Measurements have been made on the outer bremsstrahlung from different absorbers and for various sources of β-rays (2, 16, 29, 30, 32, 36), and the process has also been treated theoretically by Bethe and Heitler (3, 18). The total bremsstrahlung arising from the stopping of all the electrons in a thick plate can be calculated using the formulae of Bethe and Heitler and the β-ray energy spectrum.

In the case of an absorber of thickness less than the maximum range, it is necessary to subtract the bremsstrahlung which would be produced in the same material by those electrons which have passed through the absorber. To make such a calculation, it is necessary to determine the energy spectrum of these electrons. This was done in the following manner. The most probable energy of the electrons was obtained with the aid of Bloch's (4, 5) theory; their energy distribution was determined by an extrapolation of the data of White and Millington (35), and their number was found by a combination of these data with the results of Chadwick (7) and the absorption measurements of Varder (34).

The distribution of ThCC′ β-rays was taken as the sum of Fermi curves corresponding to partial spectra with maxima of 2.248, 1.522, 0.625, and 0.446 Mev.; the total was taken from the results of Richardson and Leigh-Smith. The Fermi curve was used in preference to other distributions, because the latest measurements on β-spectra using refined techniques have been in close agreement with Fermi distributions, especially in the higher energy portions, which are of greatest interest in bremsstrahlung calculations. The largest contribution to the bremsstrahlung is made by the partial spectrum with maximum energy 2.248 Mev., which must comprise at least 80% of the ThCC′ β-rays. Omitting the partial spectrum with a maximum energy of 0.625 Mev. (corresponding to the 1.62 Mev. level) and decreasing the intensity of the partial spectrum of maximum energy 1.522 Mev. (corresponding to the 0.726 Mev. level), from 0.14 to 0.08, in conformity with the conclusions of this work, will not therefore affect the bremsstrahlung calculations to any appreciable extent.

Initial measurements were made using source-holders of platinum foil (0.10 gm. per sq. cm.) and aluminum foil (0.17 gm. per sq. cm.). These thicknesses are not sufficient to absorb all the β-rays, some of which reached the

γ-counter wall. While it is possible to calculate the effect on the γ-counter of the bremsstrahlung arising from the source-holder, the effect due to bremsstrahlung excited in the counter wall cannot be estimated. In later measurements, therefore, all the β-rays emergent from the aluminum source-holder were absorbed in a plate of Lucite (polymethylmethacrylate). The experimental results obtained under these three sets of conditions are shown in Fig. 4, and the results of the calculation of the effect on the γ-counter of the external bremsstrahlung excited in the source-holder are given in Table V.

TABLE V

CALCULATED VALUES FOR OUTER BREMSSTRAHLUNG EXCITED IN THE SOURCE-HOLDER (PER DISINTEGRATION ThCC′)

Foil substance	Thickness, gm./sq. cm.	Outer bremsstrahlung, kev.
Platinum	0.10	23.5
Aluminum	0.17	5.6

It has been well established that the intensity of outer bremsstrahlung is proportional to the atomic number of the target substance (29, 31, 36, 2). Hence all calculations were first worked out for aluminum, and the required result was obtained merely by multiplying this by the ratio of the atomic number of the absorber to that of aluminum.

The bremsstrahlung excited in the Lucite is estimated at 0.6 kev., which together with the inner bremsstrahlung of 1.76 kev., gives a total correction when both aluminum and Lucite absorbers are present, of 8 kev.

Several factors limit the accuracy of these figures. The results of Varder, which were used to obtain the distribution curve for the transmitted β-rays, hold accurately only for the geometry which he used, since the energy distribution of the transmitted β-rays changes with angle (11). In the work of White and Millington, foils were used having thicknesses up to a maximum of 17 mgm. per sq. cm. Extrapolating their results to the thicknesses used in this work probably introduced another source of error. However, it is felt that the error in these calculations should not be greater than 15 to 20%.

Results

The experimental data obtained are shown in Fig. 4. Efficiency values of the γ-counter for ThCC′ γ-rays are plotted against the resolving time of the coincidence mixer. The upper and center curves are based on data obtained using platinum and aluminum foil source-holders, respectively. The lower curve was obtained when the β-rays transmitted through the aluminum foil were absorbed in Lucite before reaching the γ-counter. It has been corrected for absorption of the 0.726 Mev. γ-ray in the Lucite. In taking the average

value for the efficiency, as given in Column 2 of Table VI, only those points on the flat portion of the curve, i.e., for which the resolving time was greater than 1 μsec., were used.

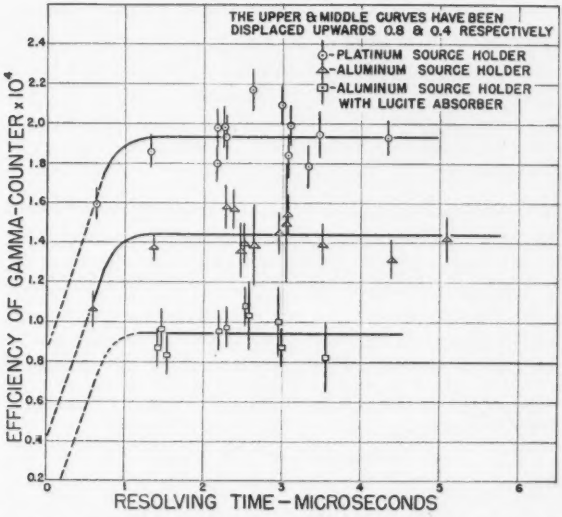

FIG. 4. *Experimental data on the efficiency of the γ-counter for γ-rays of ThCC′.*

In Table VI are given the mean values of the γ-counter efficiencies in the three cases, with the values of total γ-ray plus bremsstrahlung energy calculated from these efficiencies. Only in the third case, using an aluminum

TABLE VI

EXPERIMENTAL RESULTS ON THE TOTAL γ-RAY ENERGY OF THCC′

Calibration constant for the γ-counter: $K = (1.57 \pm 0.02) \times 10^3$

Source-holder	Efficiency of γ-counter $\bar{\epsilon}_\gamma \times 10^4$	Total γ-ray + bremsstrahlung energy, $K \cdot \bar{\epsilon}_\gamma$, Mev.	Bremsstrahlung correction,** B, Mev.	Total γ-ray energy $K \cdot \bar{\epsilon}_\gamma - B$, Mev.
Pt	1.14 ± 0.02	0.178 ± 0.007	0.026	0.152 ± 0.007
Al	1.04 ± 0.03	0.160 ± 0.006	0.008	0.152 ± 0.007
Al*	0.94 ± 0.03	0.147 ± 0.006	0.008	0.139 ± 0.006

* *With Lucite absorber of 1.4 gm. per sq. cm.*

** *Calculated values of bremsstrahlung considered good to 20%. An unknown amount of bremsstrahlung, which originates in the wall of the counter, must be added to the first two cases.*

source-holder and Lucite screen, is the correction for bremsstrahlung known completely, hence only in this case is the value calculated for the total γ-ray energy of ThCC′ accepted.

Although the experiment was not of sufficient precision to determine the amount of bremsstrahlung accurately, at least the order of magnitude was found to be in agreement with calculated values. For example, the decrease in bremsstrahlung on changing the source-holder from platinum to aluminum, as obtained from Column 3, Table VI, is 18 ± 13 kev., which agrees in order of magnitude with that of 18 ± 6 kev. found from Column 4. This comparison neglects the difference in bremsstrahlung due to the transmitted β-rays for the two cases. According to the data of Column 5, the net bremsstrahlung due to these β-rays impinging on the wall of the γ-counter is 13 ± 13 kev., so that such a difference is small and is probably masked by the uncertainty in measurement.

The most probable error in the determination of the γ-counter efficiency for the case where the Lucite absorber was used, is 2.6%, and that for the constant of calibration is 1.3%. These give an experimental precision of about 4% in the total γ-ray energy (Column 3). Added to this will be an error of about 6% which is introduced through the assumption that a direct proportionality exists between the γ-counter efficiency and the quantum energy of the incident radiation. Hence the final result is considered to be accurate to within 10%.

Thus, the total energy of the γ-rays of ThCC′ = 0.14 ± 0.014 Mev. per disintegration of ThCC′.

Discussion of Results

Applying Gamow's hypothesis to the measurements of Lewis and Bowden, it is found that the ThC′ nucleus has two levels of excitation. These occur at 1.797 and 0.726 Mev., and may give rise to γ-rays having energies of 1.797, 1.071, and 0.726 Mev.

The measured value for the total γ-ray energy emitted per disintegration of ThC′ is 0.14 Mev., and is in good agreement with the calculated value of 0.14 Mev. (see Table III), computed on the assumption that only the 1.80 and 0.726 Mev. γ-rays originate in the ThC′ nucleus and that both are electric quadrupole. Addition of the 2.20 Mev. radiation would give a total energy of 0.200 Mev., which is in considerable disagreement with the measurements.

The present measurements indicate, therefore, that the energy level scheme for the ThC′ nucleus suggested by the Russian workers is too complex and that there is no evidence in support of the presence of a 2.20 Mev. level of excitation.

Measurements were well advanced before it was realized that some of the recorded coincidences were between the bremsstrahlung and α-particles. Therefore, as stated above, only the data obtained with an aluminum source-holder and Lucite absorber have been utilized. The first two sets of data, however, give an indication of the amount of bremsstrahlung present, and this is seen to be of the same order as the calculated amount arising from the source-holder only (Table V). A more satisfactory arrangement would have been to make the source-holder from material of low atomic number, and

thick enough to absorb all the electrons from ThC. The observations on bremsstrahlung show the importance of considering this phenomenon when the coincidence method is used to investigate γ-rays of low intensity.

Acknowledgments

The authors wish to express their gratitude to Dr. B. B. Kinsey for his suggestion of the problem, and for advice and encouragement. They are also grateful to Dr. Muriel Wales for the calculations on inner bremsstrahlung, and to Dr. L. G. Elliott for his interest and provision of the radiothorium source.

References

1. ALICHANOV, A. I. and DZELEPOV, V. P. Compt. rend. acad. sci. U.R.S.S. 20 : 113. 1938.
2. ARCIMOVITCH, L. A. and CHRAMOV, V. A. Bull. acad. sci. U.R.S.S. Série Phys. 5-6 : 757. 1938.
3. BETHE, H. and HEITLER, W. Proc. Roy. Soc. London, A, 146 : 83. 1934.
4. BLOCH, F. Ann. Physik, 16 : 285. 1933.
5. BLOCH, F. Z. Physik, 81 : 363. 1933.
6. BRADT, H. and SCHERRER, P. Helv. Phys. Acta, 16 : 259. 1943.
7. CHADWICK, J. Deut. Phys. Ges. Verh. 16 : 383. 1914.
8. DEUTSCH, M. and ELLIOTT, L. G. Phys. Rev. 62 : 558. 1942.
9. DROSTE, G. F. v. Z. Physik, 100 : 529. 1936.
10. DUNWORTH, J. V. Rev. Sci. Instruments, 11 : 167. 1940.
11. EDDY, C. E. Proc. Cambridge Phil. Soc. 25 : 50. 1929.
12. ELLIS, C. D. Proc. Roy. Soc. London, A, 138 : 318. 1932.
13. ELLIS, C. D. Proc. Roy. Soc. London, A, 143 : 350. 1933.
14. FLAMMERSFELD, A. Z. Physik, 114 : 227. 1939.
15. GAMOW, G. Nature, 126 : 397. 1930.
16. GRAY, J. A. Proc. Roy. Soc. London, A, 85 : 131. 1911.
17. GRAY, L. H. Proc. Roy. Soc. London, A, 159 : 263. 1937.
18. HEITLER, W. The quantum theory of radiation. Oxford University Press, London. 1944.
19. HULME, H. R. Proc. Roy. Soc. London, A, 138 : 643. 1932.
20. JOHANSSON, A. Arkiv. Mat. Astron. Fysik, A, 34, No. 9 : 1. 1947.
21. KNIPP, J. K. and UHLENBECK, G. E. Physica, 3 : 425. 1936.
22. LATYSCHEV, G. D. and KULCHITSKY, L. A. J. Phys. U.S.S.R. 4 : 515. 1941.
23. LEWIS, W. B. and BOWDEN, B. V. Proc. Roy. Soc. London, A, 145 : 235. 1934.
24. RICHARDSON, H. O. W. and LEIGH-SMITH, A. Proc. Roy. Soc. London, A, 16. : 391. 1937.
25. ROSENBLUM, S. and VALADARES, M. Compt. rend. 194 : 967. 1932.
26. RUTHERFORD, LORD, WYNN-WILLIAMS, C. E., and LEWIS, W. B. Proc. Roy. Soc. London, A, 133 : 351. 1931.
27. RUTHERFORD, LORD, WYNN-WILLIAMS, C. E., LEWIS, W. B., and BOWDEN, B. V. Proc. Roy. Soc. London, A, 139 : 617. 1933.
28. SHENSTONE, A. G. and SCHLUNDT, H. Phil. Mag. 43 : 1038. 1922.
29. SIZOO, G. J., EIJKMAN, C. and GROEN, P. Physica, 6 : 1057. 1939.
30. STAHEL, E. and COUMOU, D. J. Physica, 2 : 707. 1935.
31. STAHEL, E. and GUILLISSEN, J. J. phys. radium, 1 : 12. 1940.
32. STAHEL, E. and KIPFER, P. Helv. Phys. Acta, 9 : 492. 1936.
33. TAYLOR, H. M. and MOTT, N. F. Proc. Roy. Soc. London, A, 138 : 665. 1932.
34. VARDER, R. W. Phil. Mag. 29 : 725. 1915.
35. WHITE, P. and MILLINGTON, G. Proc. Roy. Soc. London, A, 120 : 701. 1928.
36. WU, C.-S. Phys. Rev. 59 : 481. 1941.
37. YUKAWA, H. and SAKATA, S. Sci. Papers Inst. Phys. Chem. Research, Tokyo, 31 : 187. 1937.

CANADIAN JOURNAL OF RESEARCH

Notes on the Preparation of Copy

GENERAL:—Manuscripts should be typewritten, double spaced, and the **original and one extra copy** submitted. Style, arrangement, spelling, and abbreviations should conform to the usage of this Journal. Names of all simple compounds, rather than their formulae, should be used in the text. Greek letters or unusual signs should be written plainly or explained by marginal notes. Superscripts and subscripts must be legible and carefully placed. Manuscripts should be carefully checked before being submitted, to reduce the need for changes after the type has been set. If authors require changes to be made after the type is set, they will be charged for changes that are considered to be excessive. **All pages, whether text, figures, or tables, should be numbered.**

ABSTRACT:—**An abstract of not more than about 200 words, indicating the scope of the work and the principal findings, is required.**

ILLUSTRATIONS:

(i) *Line Drawings:*—All lines should be of sufficient thickness to reproduce well. Drawings should be carefully made with India ink on white drawing paper, blue tracing linen, or co-ordinate paper **ruled in blue only**; any co-ordinate lines that are to appear in the reproduction should be ruled in black ink. Paper ruled in **green, yellow, or red should not be used** unless it is desired to have all the co-ordinate lines show. Lettering and numerals should be neatly done in India ink preferably with a stencil (**do not use typewriting**) and be of such size that they will be legible and not less than one millimeter in height when reproduced in a cut three inches wide. All experimental points should be carefully drawn with instruments. Illustrations need not be more than two or three times the size of the desired reproduction, but the ratio of height to width should conform with that of the type page. **The original drawings and one set of small but clear photographic copies are to be submitted.**

(ii) *Photographs:*—Prints should be made on glossy paper, with strong contrasts; they should be trimmed to remove all extraneous material so that essential features only are shown. Photographs should be submitted **in duplicate**; if they are to be reproduced in groups, one set should be so arranged and mounted on cardboard with rubber cement; the duplicate set should be unmounted.

(iii) *General:*—**The author's name, title of paper, and figure number should be written in the lower left-hand corner (outside the illustration proper) of the sheets on which the illustrations appear.** Captions should not be written on the illustrations, but typed on a separate page of the manuscript. All figures (including each figure of the plates) should be numbered consecutively from 1 up (arabic numerals). **Each figure should be referred to in the text.** If authors desire to alter a cut, they will be charged for the new cut.

TABLES:—Titles should be given for all tables, which should be numbered in Roman numerals. Column heads should be brief and textual matter in tables confined to a minimum. **Each table should be referred to in the text.**

REFERENCES:—**These should be listed alphabetically by authors' names, numbered in that order, and placed at the end of the paper.** The form of literature citation should be that used in the respective sections of this Journal. **Titles of papers should not be given in references listed in Sections A, B, E, and F, but must be given in references listed in Sections C and D.** The first page only of the references cited in papers appearing in Sections A, B, and E should be given. **All citations should be checked with the original articles.** Each citation should be referred to in the text by means of the key number; in Sections C and D the author's name and the date of publication may be included with the key number if desired.

The *Canadian Journal of Research* conforms in general with the practice outlined of the *Canadian Government Editorial Style Manual*, published by the Department in Public Printing and Stationery, Ottawa.

Reprints

Fifty reprints of each paper without covers are supplied free. Additional reprints, if required, will be supplied according to a prescribed schedule of charges. On request, covers can be furnished at cost.